Electrostatic Fields without Singularities: Theory, Algorithms and Error Analysis

Marco Pellegrini*

July 23, 1998

Abstract

The following problems which arise in the computation of electrostatic forces and in the Boundary Element Method are considered. Given two convex interior-disjoint polyhedra in 3-space endowed with a volume charge density which is a polynomial in the Cartesian coordinates of R^3, compute the Coulomb force acting on them. Given two interior-disjoint polygons in 3-space endowed with a surface charge density which is polynomial in the Cartesian coordinates of R^3, compute the normal component of the Coulomb force acting on them. For both problems adaptive Gaussian approximation algorithms are given, which, for n Gaussian points, in time $O(n)$, achieve absolute error $O(c^{-\sqrt{n}})$ for a constant $c > 1$. Such a result improves upon previously known best asymptotic bounds. This result is achieved by blending techniques from integral geometry, computational geometry and numerical analysis. In particular, integral geometry is used in order to represent the forces as integrals whose kernel is free from singularities.

1 Introduction

1.1 The Problem

Coulomb's law states that a particle of charge q_1 at position p_1 exerts over a particle of charge q_2 at position p_2 a force $\vec{F}_{12}$ given by:

$$\vec{F}_{12} = \frac{q_1 q_2}{4\pi\epsilon_0 |p_1 - p_2|^2} \frac{p_1 - p_2}{|p_1 - p_2|},$$

*Istituto di Matematica Computazionale del CNR, Via S.Maria 46, 56126-Pisa (Italy). e-mail: pellegrini@imc.pi.cnr.it

where ϵ_0 is the electric permeability of free space, and in the Gaussian unit system $4\pi\epsilon_0 = 1$ [Jac75]. Suppose now that we are given two fully dimensional convex bodies B_1 and B_2 endowed with volume charge density functions ρ_1 and ρ_2 respectively. We can formulate the total force acting on one of the two bodies by integrating Coulomb's law over the points of the two bodies:

$$\vec{F}_{12} = \int_{p_1 \in B_1} \int_{p_2 \in B_2} \frac{\rho_1(p_1)dp_1\rho_2(p_2)dp_2}{4\pi\epsilon_0 |p_1 - p_2|^2} \frac{p_1 - p_2}{|p_1 - p_2|}. \tag{1}$$

We will refer to integral (1) also as the volume-to-volume integral. If we are given two flat convex bodies P_1 and P_2 endowed with surface charge density functions σ_1 and σ_2, the total force acting on one of the two bodies is given by the following integral:

$$\vec{F}_{12} = \int_{p_1 \in P_1} \int_{p_2 \in P_2} \frac{\sigma_1(p_1)dp_1\sigma_2(p_2)dp_2}{4\pi\epsilon_0 |p_1 - p_2|^2} \frac{p_1 - p_2}{|p_1 - p_2|}. \tag{2}$$

We will refer to integral (2) also as the surface-to-surface integral. This integral (2) has relevance in *direct* electrostatic problems, where the density of charge is known, however it is probably more useful in *inverse* electrostatic problems, where the actual distribution of charge is approximated by a truncated functional series. In such a case the density functions σ_1 and σ_2 in integral (2) are elements in the functional basis. Formula (1) can be seen as a generalization of (2). We obtain other integrals considered in the literature when we allow one of the two bodies to degenerate into a point (point-to-surface and point-to-volume integrals).
Analytic solutions of integral (1) and (2), or of similar integrals derived for the electrostatic potential, are rarely possible, or, whenever possible, might require complex and tedious symbolic calculations. Thus often numerical integration is the method of choice. The main problem in a numerical evaluation of integrals (1) and (2) is that the kernel function is diverging within the integration domain when the closures of the bodies B_1 and B_2 (or the relative closures of P_1 and P_2) have points in common.

1.2 Overview of results in this paper

In this paper we first manipulate integrals (1) and (2) with the objective of obtaining an equivalent formulation more suitable for numerical integration. Then we describe an approximation algorithm and we give the error analysis of the proposed algorithm. Before we give more details of the techniques used and the results obtained we will briefly survey the current state of the art.

1.3 Previous work: numerical integration

1.3.1 Point-singularity and Collocation method

Approximating an integral via the evaluations of the integrand function at selected points in the domain of integration is the classical problem of numerical integration [DR75] [KE97, Ee92]. The situation when the integrand function has singularities inside the domain of integration or on its boundary has been the subject of a substantial recent research effort (see e.g. [Duf82] [LM80] [Sch94b] and a recent survey [LC94]).

A problem often considered is when the domain is a simplex or a cube in d-dimensional space with a point singularity at a vertex (conventionally taken as the origin) [Duf82, LM80, Sch94b]. Lyness [Lyn76, Lyn78], and Lyness and Monegato [LM80] show that for singularities of the form $|p|^{\alpha}$, where $|p|$ the distance of a point p from the origin and α a real number greater than $-d$, the error of a proposed recursive quadrature rule is expressed as an asymptotic expansion. Duffy [Duf82] showed that, for a class of singularities which includes the one described above, a certain variable transformation reduces the order of the singularity so that standard product integration rules may become applicable. Finally, for a vast class of functions with a singularity at the origin Schwab [Sch94b] proves that a proposed adaptive quadrature rule achieves an exponential error bound.

The theory in [LM80, Sch94b] does not seem to extend immediately to the case when the set of singularities has dimension two (e.g. two polyhedra sharing a face) or one (e.g. two triangles sharing an edge), which are the cases where integrals (1) and (2) have the worst singular behaviour. A straightforward application of the transformation proposed by Duffy does not produce immediately the desired softening of singularities on (1) and (2). However, if one of the two bodies degenerate into a point, then the point-to-surface or point-to-volume integral that is left from (1) and (2) fits in the framework of [Duf82, LM80, Sch94b]. This type of integrals with a point singularity are useful in the context of the Collocation method for the solution of integral equations of conductors [Zho93]. An extensive treatment of singularities and quasi-singularities within the Collocation methods can be found in [Sch94a]. A heuristic method is described in [Geo91].

1.3.2 Integrals of the Galerkin boundary element method

Due to their importance for the boundary elements method (BEM for short) [Zho93, BL73, CS80] singular integrals similar to (2) have received special attention in the recent literature (see e.g. [Gue92], [SW92a], [SW92b]).

Hackbusch and Sauter [HS93] consider a class of integrals which include integral (2) and obtain an equivalent formulation where the domain of integration is 3-dimensional and the kernel function has no singularities in the domain of integration. A tensor-product Gauss formula is used to evaluate the integral, however an error analysis of the proposed method is not given. Sauter and Schwab [SS96] consider the same class of integrals and derive an equivalent formulation where the domain of integration is 4-dimensional and the kernel function does not diverge within the domain of integration. It is proved in [SS96] that the proposed tensor-product Gauss formula gives an error $O(exp(-b\sqrt[4]{n}))$ where n is the number of Gaussian points used by the algorithm, and b is a constant.

An issue related to the computation of integrals in the BEM is the structure of resulting stiffness matrix. The interplay between geometric meshing, approximation of the entries of the stiffness matrix, block structure of the matrix itself, and fast iterative solution methods is studied in [vPS96], [HLS95] and [SK96]. In this paper we do not address such issue, which will be central in future research.

1.4 Fast multipole methods for point-to-volume integrals

The fast multipole method [Rok83] has found in recent years many applications to the solution of integral equations [Rok83], to the n-body problem [GR87] [1], and in numerical integration of PDE [MGM95].

Mayo [May92] has proposed a method for evaluating volume integrals of potential theory by considering the equivalent Poisson equation. Such equation is then discretized using a finite difference approach. The weighted sum of the values of the potential field at nodal points within the domain of integration is used as final approximate value of the integral. This approach is greatly enhanced by the use of a fast Poisson solver such as those based on multipole expansions [MGM95] [GGM93].

Integrals considered in [May92] are for the potential field (not the electrostatic field) and correspond to the case where one body degenerates into a point (point-to-volume integrals). However, the second body can have arbitrary shape as long as we have a routine to decide whether a nodal point is interior or exterior.

1.5 A new approach based on integral geometry

The basic intuition behind the approach used in this paper is that electrostatic forces act along *straight lines* in a homogeneous medium, and moreover the module of Coulomb force is akin to one of the forms of the differential measure of lines in 3-space. As a consequence, it is possible to define the

[1] See related work on the n-body problem in [App85] [BH86] [Gre88] [Zha87] [CK95] [PRT92].

electrostatic force produced by extended bodies in 3-space as an integral over a set of lines in 3-space. Such a representation is independent of any coordinate system for lines. Afterwards we choose a convenient way of representing lines in 3-space so to obtain for integral (1) a representation with a regular kernel. The theory developed for fully dimensional bodies is then used to support the derivation of a similar representation for the integral (2) relative to two flat bodies. We obtain integrals whose domain is the unit sphere of directions, while the value of the kernel at a given direction is associated to the orthogonal projection of the bodies B_1 and B_2 (resp. P_1, P_2) in that direction. The new volume-to-volume and surface-to-surface integrals are approximated by a weighted sum of values of the kernel. The kernel is evaluated for a fixed direction by using techniques from computational geometry, while a finite set of directions is chosen with a Gaussian adaptive cubature rule. The main result of this paper is Corollary 1 which states that the value of integral (1) and the value of the normal component of integral (2) can be approximated in time $O(n)$, where n is the number of Gaussian points used, while achieving an error $O(c^{-\sqrt{n}})$ for a constant $c > 1$.

1.6 Comparison with previous results: theoretical aspects

Our result improves the error bound on approximating integral (2) from $O(exp(-\sqrt[4]{n}))$, as in [SS96], to $O(exp(-\sqrt{n}))$, where n is the number of Gaussian points used. However, the improved dependency on n has to be weighted against the possible increase in the time needed to compute the kernel for each Gaussian point. This trade-off does not effect the asymptotic result but might impact on the actual running time for small values of n.
The theory in [SS96] and [HS93] applies to integral with singularities depending on a parameter which may assume a continuum of values, thus it has the potential for modeling a large class of phenomena. With our approach we are able to treat singularities that can be interpreted geometrically. We could find such interpretation for integrals of the electrostatic field (this paper and [Pel96]), integrals of the potential field [Fin96] and integrals in radiosity [Pel97]. At the moment we do not have such an interpretation for, say, dipole integrals or those integrals arising in hypersingular integral equations.
As for the integral (1), representing the force between two extended bodies in 3-space, we could not find any method in literature with an error bound on its accuracy. As mentioned before, the method of Mayo [May92] computes the potential at a single point in space induced by a spatial charge distribution (point-to-volume).
A remarkable fact is that the theory, algorithms and error analysis we de-

velop for the volume-to-volume case (integral (1)) is actually simpler that the equivalent for the surface-to-surface case (integral (2)). This is in sharp contrast with most methods where increase in dimension entails a more complex treatment. Sometimes 3-dimensional models are analyzed with the additional assumption that one dimension is much smaller then the others (thin-plate assumption) (see e.g. [Sch95]); no such assumption is needed in our treatment.

Results in [HS93, SS96] are obtained using the concepts of *Cauchy principal value* and *Hadamard finite part integral* [DR75, HS93]. Intuitively, the method of the Cauchy principal value consists in choosing a subdomain $D' \subset D$ of the integration domain D such that the singularity is in the difference $D' \setminus D$, then the limit of the integral over D' is taken, as D' tends to D. In the Hadamard finite part integral, besides the above described limiting process, the function itself is modified by subtracting the value of an Hölder continuous factor of the kernel, evaluated at the singular point. Our approach is rather different. We manipulate only the kernel function by using several formulations of the differential measure of lines. Uniqueness of geometric measures for lines ensures the equivalence of integrals based on different forms of the differential measure of lines. With this approach we avoid completely limiting processes in the volume-to-volume integral. We still use limiting processes for the surface-to-surface case although not of the type described above.

1.7 Organization of the paper

In Section 2 we derive a singularity-free form for the volume-to-volume integral (1). In Section 3 we derive a singularity-free form of the surface-to-surface integral (2) which arise naturally within the Boundary Element Method. Section 4 introduces the numerical integration scheme. In Section 5 we give the error analysis of the Gaussian adaptive integration algorithm for a class of *well-behaved* integrals. In Section 6 we describe a local systems of coordinates which is used in Sections 7 and 8 to prove that our geometric integrals are well-behaved so that the analysis in Section 5 holds for them. In Section 9 we report on experiments.

2 An Integral Geometric Theory of Electrostatic Fields

In this section we present a geometric interpretation of electrostatic force fields using tools from integral geometry. We adopt an axiomatic approach. We give an integral geometric definition of a field $\vec{G}$, which we will call the *geometric field*. We will show that the geometric field satisfies Gauss's Law of flux through a closed (convex) surface. Well known arguments of electrostatics can then be invoked to base the classical theory of electrostatic fields on Gauss law [Jac75] [LL80]. The theory is developed for fully dimensional convex bodies in 3-space.

Let us denote with L an oriented line in 3 space, with $\vec{L}$ the unit vector along L and dL the differential measure of lines in 3-space. Let us consider a density function $\rho_1(p)$ defined over the points p of a compact convex body B_1, and let $\bar{\rho}_1$ be the maximum of the absolute value of $\rho_1(p)$ in B_1. Let us define for a line L the quantity $m_1(L)$:

$$m_1(L) = \int_{p \in L} \rho_1(p) dp.$$

Notice that $|m_1(L)| \leq \bar{\rho}_1 \mu(L \cap B_1)$, where μ measures the length of a segment, and equality holds for a constant density of charge. Let Q_1 be the total charge of B_1:

$$Q_1 = \int_{p \in B_1} \rho_1(p) dp.$$

The Geometric field at a point $p \notin B_1$ is defined as:

$$\vec{G}_1(p) = \int_{L \cap p \neq \emptyset} m_1(L) \vec{L} dL \tag{3}$$

The lines are considered oriented from B_1 to p, and the integral is an integral of vectors. Since we consider convex bodies, although the lines are oriented, we use in many cases the underlying set of unoriented lines when it is convenient to do so. Sometimes it is more convenient to work with the component of $\vec{G}$ is some direction $\vec{w}$, which is given by:

$$\vec{G}_1 \cdot \vec{w} = \int_{L \cap p \neq \emptyset} m_i(L)(\vec{L} \cdot \vec{w}) dL.$$

We will compare our results with those obtained through the traditional definition of the electrostatic field in the Gauss unit system (see [Jac75]).

2.1 Gauss Law.

Gauss Law states that the integral of the component of the electric field $\vec{E}(p)$ in direction $\vec{n}(p)$ normal to a closed connected surface $S = \partial B$ is equal to 4π times the total charge in the bounded connected region B enclosed by the surface S:

$$\int_{p\in S} \vec{E}\cdot\vec{n}dp = 4\pi\int_{p\in B}\rho(p)dp.$$

Let us take a convex surface S and let us parameterize the (directed) lines as a point on the surface and an (outer) direction u in the set of directions $U/2$. In these coordinates the differential element of lines is $dL = \cos\theta dpdu$, where dp is the differential element of surface area, du is the differential element of directions, and θ in the angle between the (outer) normal to $\vec{n}(p)$ and the direction u. We have that:

$$\int_{L\cap S\neq\emptyset} m_1(L)dL = \int_{p\in S}\int_{u\in U/2} m_i(L)\cos\theta dudp$$
$$= \int_{p\in S}\vec{G}(p)\cdot\vec{n}(p)dp,$$

where the last expression is the standard definition of the flux of a vector field through the surface S. Now we start from the same integral but we identify any line by a pair $L = (u,q)$ where u is the direction of L, and q is the point intercepted by L on a plane $P(u)$ of normal u and incident to the origin. Using these coordinates the differential measure of lines is $dL = du\wedge dq$ [San76]. Consider $B_1\subseteq B$. We obtain:

$$\int_{L\cap S\neq\emptyset} m_1(L)dL = \int_{L\cap B_1\neq\emptyset} m_1(L)dL =$$
$$\int_{u\in U}[\int_q m_1(u,q)dq]du =$$
$$\int_{u\in U}[\int_q[\int_{p\in L,L=L(u,q)}\rho_1(p)dp]dq]du$$
$$\int_{u\in U}[\int_{p\in B_1}\rho_1(p)dp]du = 4\pi Q_1,$$

where in the last integral the domain of q is the projection of B onto $P(u)$. To summarize, starting from the same integral we have derived two different expressions which we may therefore equate, obtaining:

$$\int_{p\in S}\vec{G_1}\cdot\vec{n}dp = 4\pi Q_1,$$

which is the statement of Gauss's law for the field $\vec{G}$.

2.2 Force acting between two convex bodies

From now on we will not distinguish any more between the geometric field $\vec{G}_i$ and the electrostatic field $\vec{E}_i$ generated by a convex body B_i. Let us denote with $\vec{F}_{12}$ the force acting between bodies B_1 and B_2. We can express this force by integrating over the *points* of B_1 the value of the electrostatic field generated by B_2 at each such point. Formally we have:

$$\vec{F}_{12} = \int_{p \in B_1} \vec{E}_2(p)\rho_1(p)dp,$$

which we expand using Formula (3) into:

$$\vec{F}_{12} = \int_{P \in B_1} [\int_{L \cap p \neq \emptyset} m_2(L)\vec{L}dL]\rho_1(p)dp.$$

Now we transpose the two integrals obtaining:

$$\vec{F}_{12} = \int_L [\int_{L \cap p \neq \emptyset, p \in B_1} m_2(L)\rho_1(p)dp]\vec{L}dL.$$

The function $m_2(L)$ in the inner integral does not depend on p, thus we can take it out of the inner integral. The inner integral that is left is $m_1(L)$. The total force acting between B_1 and B_2 is thus reduced to a single integral over the set of lines in 3-space:

$$\vec{F}_{12} = \int_L m_1(L)m_2(L)\vec{L}dL \tag{4}$$

Now we identify any line by a pair $L = (u, q)$ where u is the direction of L, and q is the point intercepted by L on a plane $P(u)$ of normal u and incident to the origin. Using these coordinates the differential measure of lines is $dL = du \wedge dq$ [San76]. We obtain the new formula:

$$\vec{F}_{12} = \int_L m_1(L(u, q))m_2(L(u, q))\vec{u}dqdu$$

Thus we can split the computation into an integration over the set $U/2$ of unoriented directions[2], and, for a fixed direction $u \in U/2$, an integration over a planar set of points. So finally:

[2] The set of directions U is represented by the unit sphere in 3-space. We obtain the set of unoriented directions by identifying antipodal points on the unit sphere.

$$\vec{F}_{12} = \int_{u \in U/2} V_{12}(u) \vec{u} du \tag{5}$$

where the kernel function V_{12} is:

$$V_{12}(u) = \int_q m_1(L(u,q)) m_2(L(u,q)) dq. \tag{6}$$

Remark. The function $V_{12}(u)$ does not diverge. This is a main advantage with respect to more traditional formulations of the force acting between two bodies that are based on integrating a kernel functions, such as $1/r^2$ or $1/r$, which diverge when r goes to zero.

3 Integrals for the Boundary Element Method

To maintain the discussion self contained we show how to derive the BEM integral from Robin's integral equation for conducting bodies. Readers familiar with the Boundary Element Method may want to skip to Subsection 3.2.

3.1 Discretization of the Robin's integral equation for conducting bodies

Robin's integral equation (7) describes the equilibrium conditions for the surface charge density $\sigma(p)$ on the surface $S = \partial D$ of a closed compact (but not necessarily connected) 3-dimensional domain D [Cad95]. In this section we show a possible discretization of Robin's integral equation resulting in a Boundary Element formulation. We are interested in showing the typical form of the entries of the stiffness matrix. Then in Subsection 3.2 we turn such entries into geometric integrals without singularities. Finally we describe the algorithm for approximating such geometric integrals and we give the error analysis.

Robin's equation for the surface charge density function $\sigma(p)$ over a surface S is the following:

$$2\pi\sigma(p) = \int_{p' \in S} \frac{\cos\theta(n(p), pp')}{r^2} \sigma(p') dp', \tag{7}$$

where $\theta(n(p), pp')$ is the angle formed by the normal $n(p)$ to S at p with the line p, p', and r is the distance between p and p'. We now consider the surface as partitioned in polygons P_i with index $i \in [1, \ldots, k]$, and we compute the force acting on each polygonal face P_i. Since the electric field is normal at any point of the polygon, and the normal direction to each polygon is constant, the resultant force is also normal to the polygon P_i. Let F_i be the modulus of the (normal) force acting on polygon P_i. We can compute F_i by using the well known relation $E(p) = 2\pi\sigma(p)$ between the module of the field and the charge density at any point of the surface S. With σ_i we denote the restriction of the function σ on P_i. We obtain:

$$F_i = \int_{p \in S} E_i(p)\sigma_i(p)dp = \int_{p \in S} 2\pi\sigma_i(p)\sigma_i(p)dp \tag{8}$$

If we use the right side side of the equation (7) we obtain:

$$F_i = \int_{p \in S} E_i(p)\sigma_i(p)dp = \tag{9}$$

$$= \int_{p \in S} \left[\sum_{j=1, i \neq j}^{k} \int_{p' \in S_j} \frac{\cos\theta(n(p), pp')}{r^2} \sigma_j(p')dp' \right] \sigma_i(p)dp \tag{10}$$

Now we expand each local density function σ_i in an orthonormal basis with unknown scalar coefficients $A_{i,h}$:

$$\sigma_i(p) = A_{i,0}\sigma_0(p) + A_{i,1}\sigma_1(p) + A_{i,2}\sigma_2(p) + \ldots$$

Denoting with $H_{i,h}$ the following integral:

$$H_{i,h} = 2\pi \int_{p \in P_i} \sigma_h(p)\sigma_h(p)dp,$$

and exploiting orthonormality[3] we obtain that formula (8) for F_i becomes:

$$F_i = H_{i,0}[A_{i,0}]^2 + H_{i,1}[A_{i,1}]^2 + H_{i,2}[A_{i,2}]^2 + H_{i,3}[A_{i,3}]^2 + \ldots$$

Expanding formula (9) for F_i we obtain:

$$F_i = \sum_j \sum_h \sum_k \int_{p \in S_i, p' \in S_j} \frac{\cos\theta(n(p), pp')}{r^2} \sigma_h(p)\sigma_k(p')A_{i,h}A_{j,k}dpdp'$$

[3] The integral of product of functions with different index is null.

The above identities are satisfied by the solution of this system:

$$H_{i,h}A_{i,h} = \sum_j \sum_k A_{j,k} \int_{p \in S_i, p' \in S_j} \frac{\cos\theta(n(p), pp')}{r^2} \sigma_h(p)\sigma_k(p')dpdp'$$

The unknowns in the resulting linear system are the values of $A_{i,h}$. The number of such variables, sometimes referred to as the "dimension" of the system, is the product of the number of polygons P_i and the number of terms of the expansion of the density functions, in case of a uniform expansion on all the patches (also known as h-Galerkin method). Alternatively we might truncate the basis expansions differently on each polygon P_i so the total number of unknown is the sum of the terms in the truncated functional expansions (also known as hp-Galerkin). The coefficients $H_{i,h}$ can be pre-computed easily with exact analytic integration. The other coefficients on the right sides of the equations are of the form:

$$C_{i,h,j,k} = \int_{p \in S_i, p' \in S_j} \frac{\cos\theta(n(p), pp')}{r^2} \sigma_h(p)\sigma_k(p')dpdp' \tag{11}$$

where the functions σ_h and σ_k are known elements of the functional basis. Next we show how we can compute such coefficients using the general techniques developed in the first part of the paper. Integrals of this form (11) fall within the class of integrals studied in [SS96]. They are obtained in that paper with a double-layer potential formulation of the equilibrium of conductors.

3.2 Integral geometric transformation

In this section we apply integral geometric transformations to the integral in (11). To simplify the notation we drop subscripts inherited from the discretization process and we consider two triangles T_1 and T_2 and known densities σ_1 and σ_2. Thus the integral we are considering is:

$$C_{12} = \int_{p \in T_1, p' \in T_2} \frac{\cos\theta(n(p), pp')}{r^2} \sigma_1(p)\sigma_2(p')dpdp' \tag{12}$$

Let us call $\phi(n(p'), pp')$ the angle formed by the line pp' with the normal to T_2 at p', Let us assume for the moment being that the cosine of such angle is not null. Multiplying and dividing in (11) by the cosine of this angle we obtain:

$$\int_{p\in T_1, p'\in T_2} \frac{1}{\cos\phi(n(p'),pp')} \frac{\cos\theta(n(p),pp')\cos\phi(n(p'),pp')}{r^2} \sigma_1(p)\sigma_2(p')dpdp'.$$

Now we can turn to a geometric integral since we have isolated an expression of dL:

$$\int_{L, L\cap T_1\neq\emptyset, L\cap T_2\neq\emptyset} \frac{1}{\cos\phi(n(p'),p,p')} \sigma_1(p)\sigma_2(p')dL \tag{13}$$

Next we express a line L in the (u,q) coordinates;

$$\int_{u\in U} \left[\int_q \frac{1}{\cos\phi(q,u)} \sigma_1(p)\sigma_2(p')dq \right] du.$$

For flat polygonal faces and a fixed direction u the value $\cos\phi(q,u)$ does not depend on q and can be taken out of the inner integral sign:

$$C_{12} = \int_{u\in U} \left[\frac{1}{\cos\phi(u)} \int_q \sigma_1(p)\sigma_2(p')dq \right] du \tag{14}$$

Let us call $K'(u)$ the kernel integral:

$$K'(u) = \frac{1}{\cos\phi(u)} \int_q \sigma_1(p)\sigma_2(p')dq \tag{15}$$

In the next subsections we will shown that the value of $K'(u)$ does not diverge for $\cos\phi(q,u)$ going to zero and that the value of the limit can be computed with a formula obtained by a limiting process starting from formula (5).

Remark. We can obtain formula (13) by considering the formula (5) in the first part of the paper applied to two prisms with basis T_1 and T_2 and by letting the height of the prisms go to zero while maintaining a consistency condition on the local charge.

Lemma 1 *The function $K'(u)$ is bounded, for every $u \in U$ where it is defined.*

Proof. Densities σ_1 and σ_2 are polynomials over bounded domains, therefore they have a well defined absolute maximum which we denote $\bar{\sigma_1}$ and

$\bar{\sigma_2}$. Let A'_{12} be the area of the intersection of the projections of T_1 and T_2 onto a plane of normal u. An upper bound for $K'(u)$ is:

$$K'(u) \leq \bar{\sigma_1}\bar{\sigma_2}(1/\cos\phi)A'_{12}$$

Now for a generic direction u with $\cos\phi \neq 0$ we have

$$1/\cos\phi = A_2/A'_2,$$

where A_2 is the area of T_2 and A'_2 is the area of the projection of T_2 onto a plane of normal u. Since always $A'_{12} \leq A'_2$ we have that the expression

$$\frac{A_2}{A'_2}A'_{12}$$

is bounded by A_2 which is a finite value independent of u. ∎

From Lemma 1 we know that $K'(u)$ is bounded for every direction u for which is defined. We obtain a real analytic extension in directions u for which $K'(u)$ is not defined by taking an extension that coincides with the limit of $K'(u)$. In this section we derive a precise formula for such limit function $K''(u)$ by applying a limit process to the theory of the electrostatic force of extended bodies in Section 2. We show the following theorem:

Theorem 1 *The entry C_{12} in the stiffness matrix defined in (11) is given by:*

$$C_{12} = \int_{u \in U} K(u)du \tag{16}$$

where,

$$K(u) = \begin{cases} K'(u) & \textit{if } \cos\theta(u) \neq 0 \textit{ and } \cos\phi(u) \neq 0 \\ K''(u) & \textit{if } \cos\theta(u) \neq 0 \textit{ and } \cos\phi(u) = 0 \\ 0 & \textit{if } \cos\theta(u) = 0 \end{cases} \tag{17}$$

Proof. When $\cos\theta(u) = 0$ the contribution of direction u to the integral (16) is null since such integral represents the normal component of the force. When $\cos\theta(u) \neq 0$ and $\cos\phi(u) \neq 0$ the derivation of Section 3.2 is valid and gives the value of the kernel $K'(u)$, as defined in (15). Finally we have shown that $K'(u)$ is always bounded so we can take its limit value $K''(u)$ of $K'(u)$ for $\cos\phi(u) \to 0$ as the real analytic extension of kernel. ∎

3.3 Real analytic extension of the kernel

In this subsection we derive formula (19) which is a representation of $K''(u)$ useful for the algorithm and the error analysis.

We consider two prisms. Prism B_1 (resp. B_2) has basis T_1 (resp. T_2) and height t. We associate the surface charge density σ_1 (resp. σ_2) to the basis and the volume charge density ρ_1 (resp. ρ_2) to the prisms according to a rule to be specified later. We consider a direction u such that $\cos\theta(u) \neq 0$ and $\cos\phi(u) = 0$.

Geometric setting for B_1. Let l be a line in direction u. The reference frame and coordinates relative to body B_1 are as follows. Let θ be the angle of l with the normal n_1 to T_1, let z be the coordinate of points on $l \cap B_1$ taking as zero the entry point of the line l in B_1. Let x be the coordinate on the normal direction $\vec{n}_1$ and let y the coordinate along the surface T_1 on the plane defined by l and $\vec{n}_1$. Let η be the coordinate on an axis orthogonal to l and n_1. In Figure 1 the cross section of B_1 at $\eta = 0$ is shown.

The following relations hold among the several coordinates relative to the same point on l: $y = x(\tan\theta)$, $z = x/(\cos\theta)$, and consequently: $y = z(\sin\theta)$. The ranges are: $0 \le x \le t$, $0 \le y \le t(\tan\theta)$, $0 \le z \le t/(\cos\theta)$. We set the following relation among surface charge density and volume charge density: $\rho(z) = \sigma(y)/t$.

Contribution of B_1 along line l. Now we give an explicit formula for the weight of l in B_1 which is given by:

$$m_1(l) = \int_{z=0}^{t/(\cos\theta)} \rho(z)dz$$

We make a change of variable in the integral. Since: $dy/(\sin\theta) = dz$, we obtain:

$$m_1(l) = \int_{y=0}^{t(\tan\theta)} (\sigma(y)/t)(dy/(\sin\theta)) = 1/(t\sin\theta)\int_{y=0}^{t(\tan\theta)} \sigma(y)dy$$

Now we expand the σ_1 function in a series of McLaurin at the origin, assuming the appropriate differentiability conditions, which are satisfied by polynomials.

$$m_1(l) = 1/(t\sin\theta)\int_{y=0}^{t(\tan\theta)} [\sigma(0) + y(\frac{d\sigma}{dy})_0 + \ldots]dy$$

Integrating each term separately:

$$m_1(l) = 1/(t\sin\theta)\left[y\sigma(0) + y^2/2(\frac{d\sigma}{dy})_0 + \ldots\right]_{y=0}^{t(\tan\theta)}$$

We obtain:

$$m_1(l) = 1/(t\sin\theta)[t(\tan\theta)\sigma(0) + (1/2)t^2(\tan\theta)^2(\frac{d\sigma}{dy})_0 + \ldots]$$

Letting t go to zero only the first term remains:

$$m_1(l) = \sigma(0)/(\cos\theta)$$

where $\sigma(0)$ is the density of charge at the point where l meets S_1.
Geometric setting for B_2. Now we consider the weight of the line l with respect to the second slab with normal $\vec{n}_2$ orthogonal to the direction u. Let us consider for B_2 a coordinate z on l. Notice that now l forms an angle of $\pi/2$ with the normal n_2 to T_2.

We take a coordinate ξ on an axis parallel to n_2, and a coordinate η in a direction that forms an orthogonal triple with u and $\vec{n}_2$. In Figure 2 the cross section of B_2 at $\eta = 0$ is shown To keep calculations simple we show first what happens in plane $\eta = const$, then we will integrate the formula obtained in $d\eta$ within the relevant range of values of η to obtain the final result. We consider the η coordinate fixed and we work for the moment only with the ξ and z coordinates. The limits are : $0 \leq \xi \leq t$, $Z_{1\eta} \leq z \leq Z_{2\eta}$.
Contribution of B_2 along line l. Now we compute the weight of a line l parallel to u:

$$m_2(l) = \int_{z=Z_{1\eta}}^{Z_{2\eta}} \rho_2(z,\xi)dz = \int_{z=Z_{1\eta}}^{Z_\eta} \sigma_2(z)/tdz = (1/t)\int_{z=Z_{1\eta}}^{Z_{2\eta}} \sigma_2(z)dz = (1/t)M_\eta$$

where we have denoted with M_η the integral

$$M_\eta = \int_{z=Z_{1\eta}}^{Z_{2\eta}} \sigma_2(z)dz \tag{18}$$

Since both the integration limits and the integrand are polynomials for a fixed direction u, a closed form representation of the integral M_η it is not difficult, although tedious, to derive.

Application of formula (5). Formula (11) represents the normal component with respect to T_1 of the force acting between T_1 and T_2 endowed with charge densities σ_1 and σ_2. Thus we can express the normal component of such a force using formula (5) of the first part of the paper:

$$C_{12} = \lim_{t \to 0} (\vec{n}_1 \cdot \vec{F}_{12}) =$$
$$\lim_{t \to 0} \int_{u \in U} \cos\theta [\int_q m_1 m_2 dq] du$$

We can now specialize this formula for the prisms B_1 and B_2 using the quantities pre-computed below we have:

$$\int_u \cos\theta [\int_\eta \int_\xi (\sigma_1(\xi, \eta)/\cos\theta)(1/t) M_\eta d\xi d\eta] du$$

Let us perform the simplification of the cosines and consider the innermost integral, apply McLaurin expansion and let t tend to zero.

$$\int_{\xi=0}^{t} \sigma_{1,\eta}(\xi)(1/t) M_\eta d\xi =$$
$$M_\eta (1/t) \int_{\xi=0}^{t} \left[\sigma(0) + \xi (\frac{d\sigma(\xi)}{d\xi})_0 + \ldots \right] d\xi =$$
$$M_\eta (1/t) \left[\xi\sigma(0) + \xi^2 (1/2) (\frac{d\sigma(\xi)}{d\xi})_0 + \ldots \right]_{\xi=0}^{t} =$$
$$M_\eta \sigma_{1,\eta}(0)$$

So we obtain a final integral:

$$\int_u [\int_\eta M_\eta \sigma_\eta d\eta] du$$

Thus the kernel is:

$$\int_\eta M_\eta \sigma_\eta d\eta = K''(u) \tag{19}$$

Remark. Note that $K''(u)$ is an integral on a one dimensional domain, while $K'(u)$ is an integral over a two dimensional domain.

Remark. The formula we obtain for the case $\cos\phi = 0$ has been obtained under the condition that $\cos\theta \neq 0$. On the other hand the final formula does not contain any diverging function of $\cos\theta$ so there are no numerical issues in evaluating such a formula also for directions u for which $\cos\theta = 0$. What we need to make sure is that the value obtained by the formulae of the kernel tends to zero. This is the case for $K'(u)$ since this is an area integral and, when $\cos\theta = 0$ the domain is at most 1-dimensional. This is also the case for $K''(u)$ since when both $\cos\theta = 0$ and $\cos\phi = 0$ the domain of integration is zero dimensional (a point) for non-coplanar polygons so the integral defined by $K''(u)$ tends to zero.

4 Numerical integration

In the first part of the paper (Sections 2 and 3) we have shown that some classical integrals of electrostatics can be represented in an integral geometric form (5) and (16) in such a way that the kernel functions (6) and (17) do not diverge and can be evaluated exactly. Both integrals have been reduced to an integral on the unit sphere of directions. The next step is to set up a scheme for the numerical approximation of such integrals.

Approximating an integral via a weighted sum of values of the integrand function at selected points in the domain of integration is the classical problem in numerical integration [DR75]. Several basic techniques are available for low dimensional domains (see a recent survey by Cools [Coo97]). We will mention three techniques: Monte Carlo, Quasi Monte Carlo, and Gaussian quadrature.

In numerical integration the integral $\int_D f(x)dx$ is approximated by the summation $\sum_i w_i f(x_i)$ where the discrete set of points x_i, for $i = [1, N]$ is a subset of the domain D. If we use on U coordinates $u = (\alpha, \beta)$, then we will have a differential measure $du = g(\alpha, \beta)d\alpha d\beta$, and the domain D is the image of U onto R^2 given by the coordinate system. The function f is thus the product of $g(\alpha, \beta)$ and the geometric kernel (e.g. $K(u)$ for BEM integrals or $V_{12}(u)(u \cdot w)$ for the component of the force between tetrahedra in direction w).

Monte Carlo approach. The points $u_i = (\alpha_i, \beta_i)$ are chosen uniformly at random in D. The weights are all equal to $|D|/N$. See [Pel96] for an application of Monte Carlo integration to integral (5).

Monte Carlo error bounds have a typical error bound $O(N^{-1/2})$, provided the variance of the integrand function is bounded. A bound of this form has been proved in [Pel96].

Quasi Monte Carlo approach. The points $u_j = (\alpha_i, \beta_i)$ are chosen in D so to have low discrepancy [Nie92]. The weights are all equal to $|D|/N$. See

[BP97] for an application of Quasi Monte Carlo to the integral (5).
Quasi Monte Carlo error bounds have a typical error bound roughly $O(N^{-1})$ provided the total variation of the integrand function is bounded.
Gaussian quadrature and cubature formulae. The points $u_j = (\alpha_i, \beta_i)$ are chosen in D by an appropriate scaling of the zeroes of Legendre polynomials [DR75]. The weights are also derived from operations on the Legendre polynomials. We have a Gaussian quadrature rule (for dimension 1) of degree n when we choose points x_i and weights w_i so to give zero error on univariate polynomials up to degree $2n-1$.

In the second part of the paper (Sections 4.1, 5 and 6) we describe an adaptive cubature Gaussian algorithm for evaluating (5) and (16) with error $O(c^{-\sqrt{N}})$ for a constant $c > 1$.

4.1 Adaptive Gaussian Cubature Algorithm

We shall first describe the algorithm for approximating BEM integral (16). In Section 8, we shall derive the algorithm for integral (5) and its analysis.

The main idea is to study the kernel function $K(u)$ so to isolate regions of the unit sphere U where $K(u)$ is determined by a combinatorially fixed set of geometric features of the input triangles. Then each such region is refined into sub-domains so to obtain (i) a good parameterization of the integration sub-domain, (ii) good smoothness properties of the integrand function.

First we show how we derive the exponential error bound from well established theorems in numerical integration, provided that some properties hold for the problem at hand. Secondly we prove that such properties actually hold. The description of the algorithm is carried out together with its error analysis.

5 Error Analysis

5.1 From two dimensions to one dimension

We relate the error of a quadrature product Gauss rule to the error in the evaluation of restrictions of the function by 1-dimensional Gauss quadrature rule. Here we borrow Proposition 6 and 7 (page 23-26) from [vPS96] (see also [Str71] pages 137-148). Note however that in [vPS96] the space of integration is 4 dimensional while here it is two dimensional.

Lemma 2 *Let $f(x,y)$ be a continuous function of two variables with $x \in [-a,+b] = \Omega_1$, $y \in [-c,+d] = \Omega_2$. Let $\mathcal{I}_1$ be the integral operator on the first variable, $\mathcal{I}_2$ the integral operator on the second variable and $\mathcal{I}$ the* *bidimensional integral operator. Let*

$$\mathcal{I}f = \mathcal{I}_1\mathcal{I}_2 f = \int_{\Omega_1}\int_{\Omega_2} f(x,y)dxdy$$

Let Q_1 be a quadrature rule for Ω_1 and Q_2 a quadrature rule for Ω_2, $\mathcal{E}$ the error operator, then:

$$\begin{aligned}&|\mathcal{E}f| = |(\mathcal{I}f - Q_1Q_2f)| \leq \\ &|\Omega_1|(\max_{x\in\Omega_1}|(\mathcal{I}_2 - Q_2)f_x(y)|) + |\Omega_2|(\max_{y\in\Omega_2}|(\mathcal{I}_1 - Q_1)f_y(x)|)\end{aligned}$$

where $f_x(y)$ and $f_y(x)$ are restrictions of $f(x,y)$ on the first and second variable.

Proof. See proposition 6 in [vPS96]. ■

5.2 Gaussian error in one dimension

We shall use the following result of Davis [DR75] that relate the error of a Gaussian quadrature rule to the size of the region where the integrand function has an analytic extension in the complex plane (formula 4.6.1.11 in [DR75] (page 312) also Proposition 5 in [vPS96]):

Lemma 3 *Let $f(x)$ be real analytic in $[-1,1]$ and admit an analytic continuation $f(z)$ with $z = x + iy$ in the complex plane within a closed ellipse $\mathcal{S}$ with foci at $+1, -1$ and semi-axis sum γ, then:*

$$|\mathcal{E}(f)| = |\mathcal{I}f - Q_nf| \leq c\gamma^{-2n}\max_{z\in\partial\mathcal{S}}|f(z)|$$

where $\mathcal{I}f = \int_{-1}^{1} f(x)dx$ and Q_nf is the n-points Gaussian quadrature rule.

5.3 Well-behaved integrals

This concept provides the link between the general error bounding lemmas of the previous sub-sections and the BEM-integrals we consider.

Definition 1 *Integral:*

$$\int_{u\in U} f(u)du$$

is **well-behaved** *if it can be represented as:*

$$\sum_j \int_{u\in D_j} f_j(u)du,$$

where for each j, $D_j \subset U$; and for each j we can find a local system of reference LSR_j of parameters α_j and β_j such that:

1. *In LSR_j,*

$$D_j = I_{j,\alpha} \times I_{j,\beta} = [\alpha_{j,0}, \alpha_{j,1}] \times [\beta_{j,0}, \beta_{j,1}]$$

That is, D_j is mapped to a bounded rectangular domain in LSR_j.

2. *By substitution $f_j(u)$ is mapped to $f_j(\alpha_j, \beta_j)$ and we have the invariant differential element of directions $du = g_j(\alpha_j, \beta_j) d\alpha_j d\beta_j$.*

3. *For every $\bar{\alpha} \in I_{j,\alpha}$, the restriction $f_j(\bar{\alpha}, \beta_j) g(\bar{\alpha}, \beta_j) : I_{j,\beta} \to R$ admits an analytic extension in an open rectangle $Rect(\bar{\alpha})$ of the complex plane which contains strictly I_β.*

4. *Fore every $\bar{\beta} \in I_{j,\beta}$, the restriction $f_j(\alpha, \bar{\beta}_j) g_j(\alpha, \bar{\beta}) : I_{j,\alpha} \to R$ admits an analytic extension in an open rectangle $Rect(\bar{\beta})$ of the complex plane which contains strictly I_α.*

By set A strictly containing B we mean that A contains B and the boundary of A is disjoint from the boundary of B.

The following two lemmas are central in the proof of the error bound:

Lemma 4 *Integral (16) is well-behaved.*

Proof. Discussion in Section 6 constitutes the proof of this lemma.

Lemma 5 *Integral (5) is well-behaved.*

Proof. Discussion in Section 6 together with the modifications and simplifications in Section 8 constitutes the proof of this lemma.

5.4 Putting things together

Lemmas 2, 3 and 1 imply the following result:

Theorem 2 *A well-behaved integral can be approximated using $O(n)$ Gaussian point while achieving error $O(c^{-\sqrt{n}})$ for some $c > 1$.*

Proof. It is sufficient to prove the exponential bound for each D_j separately, since the number of such regions is independent of the number of Gaussian points used, and is bounded by a (small) constant. We drop the subscript j for the rest of this section. We consider for each $\bar{\alpha}$ the rectangle $Rect(\bar{\alpha})$ and we shift and scale it so that the included interval I_β coincides with the interval $[-1, 1]$. Let us call the scaled rectangle $ScRect(\bar{\alpha})$. Consider the intersection of all the scaled rectangles for all $\bar{\alpha} \in I_\alpha$:

$$IntScRect_\alpha = \bigcap_{\bar{\alpha} \in I_\alpha} ScRect(\bar{\alpha})$$

Such a rectangle $IntScRect_\alpha$ contains strictly the real closed interval $[-1, 1]$, therefore we can find an ellipse of semi-axis sum $c > 1$ which strictly contains $[-1, 1]$ and is strictly contained in $IntScRect_\alpha$. Therefore the value of the function f on the boundary of the ellipse is bounded. Let us call M the maximum of the function on the boundary of the ellipse. Plugging M and c in Lemma 3 we obtain a bound on the error of computing the Gaussian approximation of the integral of a α-restriction of f. Since this bound holds for every $\bar{\alpha}$ it is also a bound on the maximum error of an α-restriction. Such a bound multiplied by $|\beta_0 - \beta_1|$ gives the first term of the error in Lemma 2. A symmetric argument is used for the second error term in Lemma 2. This concludes the proof of the theorem. ∎

From Theorem 2, Lemma 4 and Lemma 5, it follows

Corollary 1 *Integrals (5) and (16) can be approximated using $O(n)$ Gaussian point while achieving error $O(c^{-\sqrt{n}})$ for some $c > 1$.*

6 Domain decomposition and choice of coordinates

In this section we show a specific choice of coordinates in which we express the geometric entities of the first part of the paper. We thus establish the property point (1) for the sub-domains of a well-behaved integral. We give a specific form to the differential measure on the unit sphere (point (2)). Moreover we prepare the setting for the proof of property 3 and 4 to be carried out in Section 7.

6.1 On the vertices of the integration domain

Let us call (x, y, z) the coordinates of a point p in an absolute Cartesian reference system. And let $q = (X, Y)$ represent the coordinates of the point on a plane $P(u)$ of normal direction u. Consider the formula for the BEM integral:

$$C_{12} = \int_{u \in U/2} \left[\frac{1}{\cos \phi} \int_q \sigma_1(q) \sigma_2(q) dq \right] du$$

Let T_1 and T_1 be triangles in 3-space, U the sphere of directions, $U/2$ the sphere of directions with identified opposite directions. With $T_i(u)$ we denote the projection of T onto the plane $P(u)$. Let $\sigma_1(x, y, z(x, y))$ be the density function associated with triangle T_1, and $\sigma_2(x, y, z(x, y))$ be function associated with triangle T_2. We consider the image of such functions on the plane XY, given by: $f_i = \sigma_i(x(X, Y), y(X, Y), z(x(X, Y), y(X, Y) = f_i(X, Y)$, $i \in \{1, 2\}$. Thus the function we want to integrate in the inner integral is $f_{12}(X, Y) = f_1(X, Y) f_2(X, Y)$. The domain of integration is the set $T_1(u) \cap T_2(u)$ which is a convex polygon on $P(u)$. Let us call $Vert(u) = \{(X_0, Y_0), ..., (X_k, Y_k)\}$ the collection of its vertices in counter-clockwise order.

Lemma 6 *The integral*

$$A_{12}(u) = \int_q \sigma_1(q)\sigma_2(q)dq \tag{20}$$

is expressible as a polynomial in the coordinates of points in $Vert(u)$ in the XY local reference system.

Proof. The objective is to express the inner integral as a function of the coordinates of points in $Vert(u)$. We use Green's formula on the plane stating that, for functions h and k

$$\int_D (\frac{\partial h}{\partial x} - \frac{\partial k}{\partial y}) dxdy = \int_{\partial D} kdx + hdy \tag{21}$$

We set $k = -(1/2) \int f_{12}(X, Y)dX$ and $h = (1/2) \int f_{12}(X, Y)dY$. Thus $f_{12}(X, Y) = (\partial k/\partial X) - (\partial h/\partial Y)$. Let us consider the right hand side of Green's formula. The right hand side can be computed over a polygonal chain by summing the contribution of each segment, let us consider w.l.o.g the first edge. Switching to local parametric coordinate t

$$X = (X_1 - X_0)t + X_0$$

$$Y = (Y_1 - Y_0)t + Y_0$$

we can turn the right hand side of (21) into an integral in t and integrating in the range $[0, 1]$. What is left after the integration in t is a polynomial in the quantities X_0, Y_0, X_1, Y_1. ∎

6.2 Combinatorially invariant regions on the sphere

The set $Vert(u)$ depends on u. In this section we show how to divide the sphere U into regions such that in each region $Vert(u)$ is combinatorially invariant.

Let us consider two triangles in 3 space, T_1 and T_2. If we change u continuously, $Vert(u)$ changes from one combinatorial fingerprint to another when the projection of three vertices is collinear. Let us call a *transition curve* the locus of points in U for which three specified vertices are collinear. Every such locus is a great circle on U. The collection of such great circles form an arrangement on U and every 2-dimensional cell of such an arrangement corresponds to a set of directions for which $Vert(u)$ is combinatorially invariant. Thus one such region R_j is bounded by arcs of great circles and is a "convex" polygon in spherical geometry.

Remark 1. Note that the number of regions depends only on the six vertices of the two triangles and it is thus a constant. This is the only place in the paper where working with triangles is different from working with, say, quadrilaterals.

In order to give a more concrete feeling of the regions we discuss the case of two triangles sharing an edge in the next subsection.

6.2.1 Triangles sharing an edge

Now let us consider as an example two specific triangles sharing an edge. Let us take the triangles $T_1 = (A, B, C)$ and $T_2 = (A, B, D)$, sharing edge AB, which we place on the z-axis, as shown in Figure 3.

We denote with the square brackets [] the determinant of three points in the local coordinates of the plane on which they lay, in the given order, with the last column filled with 1. The sign of this determinant denotes the relative orientation of the three points. For a generic point $p \in R^3$ we denote with p' the point in local coordinates (X, Y) obtained by projecting p onto $P(u)$. Note that the projection of a triangle is still a triangle even in local coordinates and it is completely determined by the projections of the vertices.

Let us consider $T_1' = A'B'C'$, and the lines defined by pairs $(A'B')$, $(A'C')$ and $(B'C')$. Suppose moreover that $[A'B'C'] > 0$. The formula to compute $A_{12}(u)$ depends on the position of D' in the arrangement of the three lines defined above. Four combinatorially different projections with non zero area are shown in Figure 4. The corresponding regions (see Figure 5) on the sphere are:

Region I. $D' \in T_1'$. In this case we have $T_2' \subset T_1'$ and $Vert(u) = Vert(T_2')$. In order to have this case the following conditions must be satisfied:

$$[A'B'D'] > 0$$
$$[B'C'D'] > 0$$
$$[C'A'D'] > 0$$

Region II. Here $T_1' \subset T_2'$, thus $Vert(u) = Vert(T_1')$. This formula is used under the following conditions:

$$[A'B'D'] > 0$$
$$[B'C'D'] < 0$$
$$[C'A'D'] < 0$$

Region III. Here the edge $A'D'$ meets edge $B'C'$. The conditions for this case are:

$$[A'B'D'] > 0$$
$$[B'C'D'] < 0$$
$$[C'A'D'] > 0$$

The area $Vert(u) = \{A', B', (A'D' \cap B'C')\}$. Note that one point of $Vert(u)$ is not defined when $D'A'$ is parallel to $B'C'$.
Region IV. Here $B'D'$ meets edge $A'C'$. The conditions are:

$$[A'B'D'] > 0$$
$$[B'C'D'] > 0$$
$$[C'A'D'] < 0$$

We have $Vert(u) = \{A', B', (A'C' \cap B'D')\}$. Note that one point of $Vert(u)$ is not defined when $B'D'$ is parallel to $A'C'$.

6.3 The forbidden curve and the forbidden vector

Points in $Vert(u)$ are of two types. They are either projections of vertices of the input triangles, or they are intersections of the lines spanning projections of edges of input triangles. Points of the first type are defined for any value of u. Points of the second type might not be defined for some direction u. We prove the following lemma:

Lemma 7 *Let $p' \in Vert(u)$ be the intersection of the lines defined by pairs of points $(p'_1 p'_2)$ and $(p'_3 p'_4)$. Then p' is the projection of a point $p \in R^3$ whose coordinates are of the form:*

$$p_x = \frac{h_x}{w \cdot u} + k_x$$

$$p_y = \frac{h_y}{w \cdot u} + k_y$$

$$p_z = \frac{h_z}{w \cdot u} + k_z$$

where $w, h_x, h_y, h_z, k_x, k_y$ and k_z are polynomials in the coordinates of p_1, p_2, p_3 and p_4.

Proof. Consider (as in Figure 6) the two skew lines $p_1 p_2$ and $p_3 p_4$. They define a unique family of parallel planes which are parallel to both. Let w be the normal vector of such a family. The set of directions u for which the two lines $p_1 p_2$, $p_3 p_4$ project onto parallel lines in given by $w \cdot u = 0$, which is a linear combination of the the quantities u_x, u_y, u_z.

Now we derive the expression for the intersection of $p'_1 p'_2$ and $p'_3 p'_4$. Consider a point $p(l)$ on the line $p_3 p_4$, consider the plane through p_1, p_2 and $p_1 + u = u$. We want to find the point $p(l)$ that belongs to that plane. Such a point, when projected in direction u is the intersection of the lines $p'_1 p'_2$ and $p'_3 p'_4$. Thus it is sufficient to equate the 4-by-4-determinant of the four points to zero, i.e.,

$$[p_1, p_2, p_1 + u, p(l)] = 0.$$

Since each coordinate of the variable point is of the form: $p_x(l) = (x(p_3) - l)/(x(p_3) - x(p_4))$ (or $p_x(l) = x(p_3)$, if $x(p_3) = x(p_4)$), developing the determinant by the last row we obtain a linear equation in l. The coefficient of l is a linear combination, whose coefficients depend on p_1, p_2, p_3, p_4, of minors of the matrix $[p_1, p_2, p_1 + u]$, developing each minor on the last row we obtain a linear combination of (u_x, u_y, u_z). Going back we have that $l = g(p_1, p_2, p_3, p_4)/LC(u_x, u_y, u_z)$, therefore also the coordinates of the point $p(l)$ have the same form. The projection has no influence on the denominator. So we have proved that the denominator of the expressions for the intersection point in local coordinate is a rational polynomial whose denominator contains a linear combination of the components of u. This term must then be $w \cdot u$, since this must be a factor, but it is the only factor. ∎

We will call w the *forbidden vector* for p' and the great circle $w \cdot u = 0$ the *forbidden curve* of p' (see Figure 7). Next we state a few useful properties of regions

Lemma 8 *The closure of a region R_j does not intersect forbidden curves from vertices of its fingerprint set $Vert_j$.*

Proof. It follows from the fact that within the validity region the formula represents the integral of a bounded function over a bounded domain such a value does not diverge, therefore there can be no point in common between a regions and forbidden curves. ∎

We state without proof the next lemma.

Lemma 9 *The intersection for a region and a great circle is a connected arc of great circle.*

6.4 The sub-domains

By a spherical polygon we mean a compact subset of the sphere whose boundary is the union of arcs of great circles.

From the discussion in the first part of this section we have that the triangles T_1 and T_2 in R^3 induce on the sphere of directions an arrangement of great circles $\mathcal{A}$. Each cell R_j of such an arrangement is a spherical polygon with the property that the representation of the area function A_{12} is combinatorially invariant. Next we show how to split each such cell R_j into either quadrangular or triangular spherical polygons. Moreover we distinguish the great circle, that is the locus of point u on the sphere such that $\cos\phi = 0$. Let us call W such great circle. A few definitions:

Let e be an arc of great circle, we call $GC(e)$ the great circle spanning e. Let u_1 and u_2 be distinct points on the unit sphere, we call $SCG(u_1, u_2)$ the unique great circle incident to them. Let u_1 be a point on the unit sphere, by $OCG(u_1)$ we denote the locus of directions orthogonal to u_1, which is a great circle.

Next we show how to subdivide each region R_j into sub-domains.

Case (1). R_j does not have W on its boundary. In this case we can choose any edge e and a vertex v not adjacent to e. Let us call u_C the intersection of the great circle $GC(e)$ and $OGC(v)$. Take u_C as the "cutting pole" for R_j by drawing all great circles SCG through u_C and the vertices of R_j. This set of great circles slices R_j into a possibly empty set of spherical quadrilaterals and one spherical triangle incident on v. Note that in our construction the angle between v and u_C is $\pi/2$.

Case (2). R_j has one edge that belongs to W. Let us call such an edge e_W. In this case we must choose $e = e_W$ and perform the previous operations at

case (1). Note that the only sub domain where $\cos\phi = 0$ is the one adjacent to e_W.
To summarize we have four types of sub-domains: quadrangular and not adjacent to W, triangular and not adjacent to W, quadrangular and adjacent to W, and triangular and adjacent to W. An example is shown in Figure 8.

6.5 Local coordinate system on the unit sphere

Quadrangular sub-domains. Here we assume that the sub-domain $D = R_j$ is quadrangular, with edges e_1, e_2, e_3, e_4, where e_1 and e_3 are the result of the slicing and e_2, e_4 are portions of edges of D. Consider the intersection point u_D among the great circles $CG(e_2)$ and $GC(e_4)$. In this case the joining great circle of u_C and u_D, $GC(u_C, u_D)$, does not intersect the boundary of D since D is the intersection of a spherical wedge based on u_C and a spherical wedge based on u_D. A spherical wedge can be defined by an planar angle at the pole of the wedge. Let us consider the points u_C, u_D and the point u_{CD} that is orthogonal to both. They form a skewed triple of versors. Call u_{CDD} the point orthogonal to u_{CD} and u_D. Call u_{CDC} the point orthogonal to u_{CD} and u_C. We have two orthogonal reference frames $B = (u_{CD}, u_{CDC}, u_C)$ and $S = (u_{CD}, u_{CDD}, u_D)$. We introduce local versors and coordinate notation: Let B be a reference frame (i_B, j_B, k_B) were i_B points up, k_B to the left, and j_B towards the viewer (see Figures 9 and 10).
Projecting from j_B we see on the projection plane the x_B and z_B axis, let us call α_B the angle that the projection of u forms with the (vertical) x_B-axis, and a_B is tangent so:

$$a_B = \tan\alpha_B = \frac{u_{Bz}}{u_{Bx}}.$$

Projecting form k_B we see the x_B and y_B axis, let us call β_B the angle that the projection of u makes with the x_B axis, and b_B its tangent so:

$$b_B = \tan\beta_B = \frac{u_{yB}}{u_{xB}}.$$

Calling $H = \sqrt{1 + a_B^2 + b_B^2}$ we have:

$$u_{xB} := \frac{1}{H},$$

$$u_{yB} := \frac{b_B}{H},$$

$$u_{zB} := \frac{a_B}{H}.$$

Now we consider the slanted reference frame S. Let S be a reference frame (i_S, j_S, k_S). The x_S-axis points at the middle of the hemisphere. We obtain S by rotating B of an angle η using the x_B axis as axis of rotation. Therefore $i_B = i_S$. In matricial form:

$$\begin{pmatrix} i_S \\ j_S \\ k_S \end{pmatrix} = \begin{pmatrix} 1 & 0 & 0 \\ 0 & \cos\eta & -\sin\eta \\ 0 & \sin\eta & \cos\eta \end{pmatrix} \begin{pmatrix} i_B \\ j_B \\ k_B \end{pmatrix} \tag{22}$$

Inverting the matrix:

$$\begin{pmatrix} u_{xS} \\ u_{yS} \\ u_{zS} \end{pmatrix} = \begin{pmatrix} 1 & 0 & 0 \\ 0 & \cos\eta & \sin\eta \\ 0 & -\sin\eta & \cos\eta \end{pmatrix} \begin{pmatrix} u_{xB} \\ u_{yB} \\ u_{zB} \end{pmatrix} \tag{23}$$

We define the angles with respect to the S-reference frame:
Projecting from j_S we see in the projection plane the x_S and z_S axis, let us call α_S the angle that the projection of u forms with the (vertical) x_S-axis, and a_S is tangent so:

$$a_S = \tan\alpha_S = \frac{u_{Sz}}{u_{Sx}}.$$

Projecting form k_S we see the x_S and y_S axis, let us call β_S the angle that the projection of u makes with the x_S axis, and b_S its tangent so:

$$b_S = \tan\beta_S = \frac{u_{yS}}{u_{xS}}.$$

Dividing both sides of this identity

$$u_{yS} = (\cos\eta)u_{yB} + (\sin\eta)u_{zB}$$

by u_{xS}, we obtain:

$$b_S = (\cos\eta)b_B + (\sin\eta)a_B,$$

and therefore:

$$a_B = \frac{1}{\sin\eta}(b_S - (\cos\eta)b_B).$$

We choose as our local coordinates system for the sub-domain D the pair of parameters $(\alpha_j, \beta_j) = (b_B, b_S)$. We use the above equality to re-express H and the components of u_B in B as a function of b_B and b_S.

Triangular sub-domains. Here we assume that D is a triangular sub-domain. Therefore it is adjacent to v and, using the notation of the previous case $u_D = v$. D is the intersection of a spherical wedge based on u_C and a spherical wedge based on v. The great circle $GC(u_C, v)$ meets the boundary of D in v. On the other hand by construction v and u_C are at an angle of $\pi/2$. Therefore reference frames B and S are obtained one from the other by a rotation of $\pi/2$. Consider angles α_B and β_B. Let the range for β_B be $[\beta_0, \pi/2]$ so that the range for b_B is $[\tan\beta_0, +\infty]$. We can always choose $0 < \beta_0 < \pi/2$ (see Figures 11 and 12). We take an angle $\gamma = \beta - \beta_0$ so that calling $e = \tan\beta_0$ and $c_B = \tan\gamma$ we have:

$$c_B = \frac{b_B + e}{1 - b_B e}.$$

The range of integration now is $c_B \in [0 ... \tan(\pi/2 - \beta_0)]$ and c_B does nor diverge in this interval (although b_B would). Inverting the relation:

$$b_B := (c_B - e)/(1 + ec_B) \tag{24}$$

Now we choose as our local coordinates on the sphere $(\alpha_j, \beta_j) = (a_B, c_B)$. We can now express H, and the components of u_B as a function of a_B and c_B.

6.6 The differential measure of directions in local coordinates

From Santalo [San76] we take this form of the differential element of directions:

$$du = \frac{du_{zB} \wedge du_{yB}}{u_{xB}} \tag{25}$$

Quadrangular sub-domains In order to express du in terms of b_B and b_S we need to compute the determinant of the Jacobian J of the functions u_{yB} and u_{zB} with respect to the parameters b_B and b_S. We obtain:

$$J = -(1/\sin\eta)(1/H^4).$$

Note that for $\eta \neq 0$ this expression does not diverge for any real value of a_B and a_S. From (25) we have $du = |JH| db_B \wedge db_S$, thus

$$du = |(1/\sin\eta)(1/H^3)| db_B \wedge db_S.$$

Triangular sub-domains. We express H and the components of u_B in the B reference system in terms of a_B and c_B by using (24). We obtain

$$H = \frac{M}{(1 + ec_B)},$$

where

$$M = \sqrt{(1 + ec_B)^2(1 + a_B^2) + (c_B - e)^2}. \tag{26}$$

The determinant J of the Jacobian of the functions u_{yB} and u_{zB} with respect to parameters a_B and c_B is:

$$J = \frac{-(1 + e^2)(1 + ec_B)^2}{M^4},$$

so

$$du = |JH| dc_B \wedge da_B = \frac{(1 + e^2)(1 + ec_B)}{M^3} dc_B \wedge da_B.$$

Notice that M is the square root of a sum of squares, and it cannot be zero for any real value of e, c_B and a_B.

6.7 The projection transformation

Lemma 6 states that the area function $A_{12}(u)$ is a polynomial in the coordinates of the vertices $Vert(u)$ in local coordinates. In order to complete our description we need to give the transformation matrix which represents the projection operation in direction u. It is sufficient to give the matrix in the coordinates u_B. Denoting with the subscript P the local reference frame on $P(u)$ having u as k_P-axis:

$$\begin{pmatrix} i_P \\ j_P \\ k_P \end{pmatrix} = \begin{pmatrix} u_{Bz}u_{Bx}/G & u_{By}u_{Bz}/G & -G \\ -u_{yB}/G & u_{xB}/G & 0 \\ u_{xB} & u_{yB} & u_{zB} \end{pmatrix} \begin{pmatrix} i_B \\ j_B \\ k_B \end{pmatrix} \tag{27}$$

Where $G = \sqrt{u_{xB}^2 + u_{yB}^2}$. In terms of coordinates:

$$\begin{pmatrix} x_P \\ y_P \\ z_P \end{pmatrix} = \begin{pmatrix} u_{Bz}u_{Bx}/G & -u_{By}/G & u_{xB} \\ u_{yB}u_{Bz}/G & u_{xB}/G & u_{yB} \\ -G & 0 & u_{zB} \end{pmatrix} \begin{pmatrix} x_B \\ y_B \\ z_B \end{pmatrix} \tag{28}$$

The local coordinates of the projection are given by x_P and y_P. Using previously derived equalities we can express the components of u_B in terms of the local spherical coordinates (α_j, β_j) for sub-domain D_j.

7 Proof of Lemma 4 for BEM integrals

The functions and sub-domains described in in Section 6 satisfy by construction properties (1) and (2) of definition 1. In order to prove that properties (3) and (4) are also satisfied we need to consider several subcases.

7.1 Sub-domains not incidents to W

Let R_j be a sub-domain not incident to W. In this case the kernel of the integral is:

$$f_j(u) = \frac{A_{12}(u)}{u \cdot n_2}$$

Thus restrictions of f_j are analytic provided that restrictions of $u \cdot n_2$ and $A_{12}(u)$ are analytic and $u \cdot n_2 \neq 0$. These conditions are equivalent to requiring that: $H \neq 0$, $G \neq 0$, $u \cdot n_2 \neq 0$ and $u \cdot w_F \neq 0$ for any forbidden vector F associated with R_j. Moreover the condition $H \neq 0$ also ensures that restrictions of the function $g(u)$ associated with the differential measure of direction are analytic.

7.1.1 Coordinates (b_B, b_S)

Recalling the coordinates in Subsection 6.5 for quadrangular sub-domains we have that $H \neq 0$, corresponds to the equation: $1+a_B^2+b_B^2 = 0$. Equivalently: $1 + (\frac{1}{\sin\eta}(b_S - (\cos\eta)b_B))^2 + b_B^2 = 0$.

For a fixed value $\bar{b}_B$ we obtain two conjugated imaginary poles in the complex b_S-plane. We obtain similarly conjugated imaginary poles when we fix the $\bar{b}_S$.

Condition $G \neq 0$ corresponds to finding zeroes of $b_B^2 + 1 = 0$, thus for any fixed value $\bar{b}_S$ we have poles at $\pm i$ on the complex b_B-plane.

Note that the various transformations introduce only imaginary poles, not real ones. Let w be either a forbidden vector w_F or n_2. We show that the condition $u \cdot w = 0$ introduces only real poles. Indeed $u \cdot w = 0$ if and only if $w_x + b_B w_y + (\frac{1}{\sin\eta}(b_S - (\cos\eta)b_B))w_z = 0$. Fixing either of the variables gives a linear equation in the other variable that has one real solution. Since in the range of the closed domain D_j the function f_j is bounded, then there is a rectangle $Rect(\bar{b_S})$ in the complex b_B-plane that strictly contains the real range I_{b_S} and none of the real or complex poles. Similarly, there is a rectangle $Rect(\bar{b_B})$ in the complex b_S-plane that strictly contains the real range I_{b_B} and none of the real or complex poles. This proves properties (3) and (4) of definition 1 for rectangular sub-domains not incident to W.

7.1.2 Coordinates (a_B, c_B)

Recalling the coordinates in Subsection 6.5 for triangular sub-domains we have that $H = 0$ if and only if $M = 0$. From formula (26) we see that for a fixed value $\bar{c_B}$ we have either no roots or complex conjugated roots. For a fixed $\bar{a_B}$ equation $M = 0$ cannot have real roots in c_B. It is easy to see this by contradiction. If we suppose the existence of a real root we would have that the sum of two non negative numbers is null, which is possible only if both $(1 + ec_B)$ and $(c_B - e)$ are simultaneously zero. This is not possible for any real value of e. Thus also in this case we have two complex conjugated roots. Condition $G = 0$ is rewritten as $1 + (\frac{c_B - e}{1 + ec_B})^2 = 0$. Again, by contradiction it is easy to see that this equation cannot have real roots.

Let w be either a forbidden vector w_F or n_2. We show that the condition $u \cdot w = 0$ introduced only real poles. Indeed $u \cdot w = 0$ iff

$$(1 + ec_B)(w_x + a_B w_z) + (c_B - e)w_y = 0$$

Again this is a bilinear equation, therefore any restriction is a linear equation giving one real root. As observed before these real roots cannot be incident to the real closed domains I_{c_B} or I_{a_B}, therefore we have rectangles $Rect(\bar{c_B})$ and $Rect(\bar{a_B})$ as defined in definition 1. This proves properties (3) and (4) of definition 1 for triangular sub-domains not incident to W.

7.2 Sub-domains incident to W

In this sub-section we use generic coordinates (α, β) to denote either (b_B, b_S) or (c_B, a_B). Suppose without loss of generality that in the local coordinate system LCS_j associated with D_j we have $\cos\phi = 0$ for $\alpha = \alpha_0$.

7.2.1 Restrictions $\beta = \bar{\beta}$

The proof of the previous subsections implies that our function $f_j(u)g(u)$ is analytic in a punctured rectangle $Rect(\bar{\beta}) \setminus \{(\alpha_0, 0)\}$ in the complex plane. From Theorem 1 we know that the real univariate function $f_j(\alpha, \bar{\beta}) = K'(\alpha, \bar{\beta})$ admits at $\alpha = \alpha_0$ the real extension $K''(\alpha_0, \bar{\beta})$.

At this point we invoke a classical result in complex analysis (see e.g. [Evg66] [Con73]) stating that an analytic extension along a path on the complex plane is independent of the chosen path. Therefore the extension of $f_j(\alpha, \bar{\beta})$ as a real function is also a complex extension. This shows that our univariate restrictions of $f_j(u)g(u)$ admits a complex analytic extension within $Rect(\bar{\beta})$, thus satisfying property (4) in definition 1.

7.2.2 Restrictions $\alpha = \bar{\alpha}$

Proofs in the previous subsections show that for any $\bar{\alpha} \neq \alpha_0$ the restriction $f_j(\bar{\alpha}, \beta)g(\bar{\alpha}, \beta)$ admits a complex analytic extension in a certain rectangle on the complex plane. Thus to complete the proof it is sufficient to show that $f_j(\alpha_0, \beta) = K''(\alpha_0, \beta)$ admits an analytic extension in a rectangle of the complex β-plane. We refer to the initial treatment in Section 3.3 and to the integral geometric formula (19) for $K''(u)$.

The general flavour of this section is to follow the blueprint of the discussion in Sections 6 but on a 1-dimensional domain (the great circle W) instead of a two dimensional one (the sphere of directions).

Let us consider triangles $T_1 = (p_1, p_2, p_3)$ and $T_2 = (p_4, p_5, p_6)$ in the reference frame $J = (n_2, n_2 \times u, u)$ associated with the plane $P(u)$. Moreover we consider the distinguished points p_7, p_8 and p_9 which re the intersections of the lines spanning the edges of T_1 with the plane spanning T_2.

Note that the mapping between the B-reference frame and the J-reference frame is polynomial in the components of u_B since normalization is not needed. Since $u \cdot n_2 = 0$, the projection T_2' of T_2 in direction u is a degenerate triangle (i.e. a segment). Using the notation in Section 3.3 we have that $z_J = z$ and $y_J = \eta$.

The great circle W on the unit sphere is subdivided into arcs of great circles such that in each such arc the intersection $T_{12}' = T_1' \cap T_2'$ is combinatorially invariant, that is the relevant features of T_{12}' are defined by a combinatorially invariant set of features (vertices and edges) of the input triangles. It is easy to see that the combinatorial fingerprint of T_{12}' changes for directions in which 3 vertices or distinguished points of the input triangles are collinear, therefore the subdivision of W is just the trace on W of the transition curves defined in subsection 6.2 for the whole sphere. Therefore each such arcs coincide with sides of sub-domains as defined in subsection

(6.4).

The relevant features of T'_{12} are its end points which may be the projection of an endpoint of T_2 or the projection a distinguished point It is also possible that the projection of a vertex of T_2 is interior to T'_{12}. In this case T'_{12} is the concatenation of two combinatorial segments. We will show that, in each such arc of W, integrals (18) and (19) are defined by functions that have property (3) of definition 1. We use the following lemma:

Lemma 10 *Integral M_η defined in (18) is expressible as a rational functions in the local coordinates of endpoints of the triangles and distinguished points and a polynomial in the variable η.*

Proof. Let $\sigma_2(x_B, y_B, z_B(x_B, y_B))$ be the density function associated with the second triangle. Considering the transformation in local J-coordinate, we have $\sigma_2(p_J) = \sigma_2(x(p_J), y(p_J), z(x(p_J), y(p_J)))$. Since σ_2 is supposed polynomial in the coordinates (x_B, y_B, z_B) it is also polynomial in the components of p_J and the entries of the transformation matrix, which as observed before are polynomials in the components of u_B. Since for choice of coordinates $x_J = 0$ in the domain of interest we have that $\sigma_2 = \sigma_2(x_J, z_J) = \sigma_2(\eta, z)$ is a polynomial in the coordinates η and z and in the components of u_B. Thus the antiderivative in z has the same properties. The extremes of the integral (18) can be expressed by interpolation of the end-points of the relevant segments expressed as a linear functions of η whose coefficients are rational functions in the local coordinates of the end-points of the segment. T'_{12}. ∎

Repeating the above argument for $\sigma_1(p_B)$ we can conclude that the kernel in integral (19) is polynomial in η and so is its antiderivative. The limit of integration of (19) are expressed by the endpoints of T'_{12} in local coordinates. To summarize $K''(u)$ is expressible as a sum of rational functions of the vertices and of the input triangles and distinguished points in local J-coordinates. The directions for which the denominator of the resulting rational function is zero (forbidden directions) are directions corresponding to the edges of T_2. However $K''(u)$ is bounded for any value of $u \in W$ therefore we obtain real analytic extension by substituting the limit of the function in those directions for which the denominator of the rational function is zero.

To conclude, the mapping from the (α_0, β)-coordinates to the components of u_B introduces only imaginary poles, while the mapping from the components of u_B to $K''(u)$ does not introduce any real pole. Therefore $K''(\beta)$ admits an analytic extension in a rectangle of the complex plane that includes properly the interval I_β. This concludes the proof of Lemma 4.

8 Proof of Lemma 5 for volume-to-volume integrals

Consider two convex polyhedra B_1 and B_2 endowed with volume charge density ρ_1 and ρ_2. Let $B'_{12}(u)$ be the intersection of the projections of B_1 and B_2 onto the plane $P(u)$ of normal u. Let $M_{12}(u)$ be the planar map induced by the projections onto $P(u)$ of the edges of B_1 and B_2. The planar map $M_{12}(u)$ is composed of open faces that are either disjoint from B'_{12} or completely contained in it (we will call these faces *internal*). Each inner face is completely contained in the projection of two facets of B_1 and two facets of B_2 which we call the *covering facets*.

We prove the following lemma, which is analogous to Lemma 6.

Lemma 11 *The integral $V_{12}(u)$ defined by formula (6) is expressible as a rational function in the coordinates of the vertices of the inner faces of $M_{12}(u)$ and of the vertices of the corresponding covering facets in local coordinates.*

Proof. Let us call (X, Y, Z) the local coordinate system. The transformation from absolute coordinates to the local coordinates is linear in the local coordinates and the entries of the transformation matrix. Thus $\rho_1(X, Y, Z)$ is a polynomial in X, Y, Z. Let us consider the inner face f and let $Z = Z_1(X, Y)$, and $Z = Z_2(X, Y)$ be the equations of the planes spanning the two covering faces of B_1. Such two functions Z_1 and Z_2 are linear functions in X and Y, whose coefficients are rational functions of the coordinates of 3 vertices of the covering facets. This can be seen easily by writing the equation of the plane in the form of a determinant. The weight of a line parallel to u passing through the point $(X, Y) \in f$, relative to the first body is:

$$m_1(X, Y) = \int_{Z_1(X,Y)}^{Z_2(X,Y)} \rho_1(X, Y, Z)dZ.$$

Thus $m_1(X, Y)$ is a polynomial in X and Y whose coefficients are rational functions of the coordinates of vertices of the covering facets. A similar property holds from $m_2(X, Y)$, the weight relative to the second body. Finally using Green's formula as in Lemma 6 we can express $\int_{(X,Y)\in f} m_1 m_2 dXdY$ as a polynomial in the vertices of the face f. ∎

We subdivide the unit sphere into regions such that in each region the combinatorial fingerprint of the faces of $M_{12}(u)$ (including the covering facets) is constant. Again it is easy to show the each such region is a spherical convex polygon on the unit sphere and we can proceed as in Section 6.

The situation is rather simplified since we do not have the W great circle. On the other hand, besides the forbidden vectors introduced by vertices of inner faces resulting from intersection of skew spatial edges, we have as forbidden vectors also the normals to the covering facets. Since $V_{12}(u)$ does not diverge it is easy to conclude that also the new forbidden curves do not intersect the corresponding closed region on the unit sphere. We use the same coordinates and calculations as in Sections 6.4, 6.5, 6.6 and 6.7. Then an argument following the one in Subsection in 7.1 is used to conclude the proof of Lemma 5.

9 Experimental results

The Gaussian adaptive algorithm to compute the normal component of integral (2) using formula (14) has been implemented in C on a Pentium 100 processor running the Linux operating system and in Mathematica (version 2.2.2) under Windows '95. A more detailed description of the experiments is in [BP97].

Input. We made two sets of experiments with triangles sharing an edge. In the first experiment we set $T_1 = \{(0,0,-1),(0,0,1),(0,-1,0)\}$ and $T_2 = \{(0,0,-1),(0,0,1),(\sin A, -\cos A, 0)\}$, where the angle A assumes values $\frac{3}{4}\pi, \pi/2, \pi/4, \pi/8, \pi/16, \pi/32$. In the second experiment we set $T_1 = \{(0,0,-1),(0,0,1),(0,-1,-1)\}$ and $T_2 = \{(0,0,-1),(0,0,1),(-\sin B, 0, \cos B)\}$, where the angle B assumes values $\frac{i}{6}\pi$ for $i = 1 \ldots 5$.

The first experiment is intended to study the dependency of the algorithm on the dihedral angle between the input triangles. The second experiment is intended to study the dependency on the aspect ratio of one of the two triangles. We set the surface density functions σ_1 and σ_2 to be constant and equal to 1.

Reference value. Since we could not find analytic solutions to integral (2) or (14), we compute the reference value as follows. Starting with formulation (14) we compute the regions of the unit sphere as described in section 6.2.1 and we express the area function (20) explicitly in spherical coordinates for each region. Using Mathematica we integrate analytically in one of the variables and numerically on the second variable. The value returned by Mathematica is considered reliable up to 14 digits.

Results. We show the relative error using the notation $(n_1)n_2$ where n_1 is the number of zeroes after the decimal point, and n_2 the significant digits. In Table 1 we have the relative error for several values of the angle A as a function of the number of directions used in the numerical integration. In Table 2 we give the relative error for experiment A as a function of time.

Tables 3 and 4 give the same information for experiment B. We give plots of relative error versus number of directions in logarithmic-logarithmic scale for experiment $A = \pi/32$ (Figure 13), $A = 4\pi/3$ (Figure 14), $B = \pi/2$ (Figure 15) and $B = 5\pi/6$ (Figure 16).

Comments. In experiment A, the Gauss adaptive algorithm attains errors between 10^{-8} and 10^{-14} for 1000 directions, moreover it produces a rather smooth plot in the range $[10, 1000]$, afterwards it suffer from numerical instabilities probably due to round-off. The lower end of the error range is attained for small dihedral angles ($A = \pi/32$), while the high end is attained for angles close to $\pi/2$.

Experiment B shows errors in the range between 10^{-8} and 10^{-11} for the angles B between $\pi/6$ and $5\pi/6$, after 1000 directions . Dependency of the error on the angles A and B is weak in the middle of the range, with slightly worse performance towards the extremes of the angle range. The computing time needed to attain the best precision in each experiment is in the range 0.5 to 1 second. These times should be considered indicative only since at the moment little effort has been put in optimizing the codes. Experimental evidence is consistent with the exponential error bound predicted in Section 5 for the Gauss adaptive method.

At the moment we could not find in literature other comparable experimental data. Available data on alternative methods for computing surface-to-surface integrals [HS93, SS96, ES96] is relative to the solution of the linearized system with respect to an initial integral equation. This approach has the advantage that an analytic solution to the integral equation is found in the examples considered in [HS93, SS96, ES96], and is used as reference value. On the other hand the outcome of the experiment is influenced by the choice of meshing strategy, by the choice of the functional basis and truncation of the functional expansion. Finally, if an iterative method is used to solve the linear system, also the convergence of the iterative method influences the result. The computation of the entries of the stiffness matrix is just one of many critical steps. For the above reasons, although the preliminary experimental results are encouraging, further research is needed to integrate the proposed method of computing BEM integrals within a larger system.

10 Conclusions

In this paper we give an integral geometric interpretation of the electrostatic forces between charged bodies and charged surfaces in 3-space. The main benefit of this interpretation is that the kernel of the resulting integral does not diverge. Based on such representation, we develop approximation algo-

rithms with exponential error, which have better asymptotic bounds than previously known algorithms. Preliminary experimental data support the results of the theoretical analysis.
In the study of electrostatic fields usually powerful differential and integral methods are used, however, at the best of my knowledge, a combination of methods from integral geometry, computational geometry and numerical analysis have not been significantly used so far to derive algorithms approximating electrostatic forces. We consider the novelty of the approach as important as the specific results obtained in this paper.

11 Acknowledgments

I wish to thank Lawrence Coswar and Ken Clarkson for their observations on an early version. Two anonymous referees helped a lot with their comments and pointers at the relevant literature in numerical analysis and applied mathematics. Paolo Bientinesi has produced the experimental data, tables and plots. Part of this research has been done while visiting the International Computer Science Institute in Berkeley during August and September 1997.

References

[App85] A. W. Appel, *An efficient program for many-body simulations*, SIAM J. Sci. Statist. Comput. **6** (1985), 85–103.

[BH86] J. Barnes and P. Hut, *A hierarchical $O(n \log n)$ force-calculation algorithm*, Nature **324** (1986), 446–449.

[BL73] K.J. Binns and P.J. Lawrenson, *Analysis and computation of electric and magnetic field problems*, Pergamon Press, Oxford, 1973.

[BP97] P. Bientinesi and M. Pellegrini, *Electrostatic fields without singularities: implementations and experiments*, Tech. Report IMC B4-97-16, Istituto di Matematica Computazionale del CNR, Via Santa Maria 46, Pisa, Italy, November 1997, www.imc.pi.cnr.it/ marcop/papiri/paolo-report.ps.

[Cad95] R. Cade, *On discontinuous solutions of the integral equations of electrostatics*, IMA Journal of Applied Mathematics **55** (1995), 205–220.

[CK95] P. B. Callahan and S. R. Kosaraju, *A decomposition of multidimensional point sets with applications to k-nearest-neighbors and* *n-body potential fields*, Journal of the ACM **42** (1995), no. 1, 67–90.

[Con73] J.B. Conway, *Functions of one complex variable*, Springer Verlag, 1973.

[Coo97] R. Cools, *The approximation of low-dimensional integrals: available tools and trends*, Numerical Mathematics, Proceedings of the 15th IMACS World Congress on Scientific Computation, Modelling and Applied Mathematics (Berlin) (A. Sydow (ed.), ed.), vol. 2, Wissenschaft & Technik Verlag, August 1997, www.cs.kuleuven.ac.be/publicaties/rapporten/tw/TW259.ps.gz, pp. 469–474.

[CS80] M.V.K. Chiari and P.P. Silvester (eds.), *Finite elements in electrical and magnetic field problems*, John Wiley and Sons, New York, 1980.

[DR75] P. J. Davis and P. Rabinowitz, *Methods of numerical integration*, Academic Press, New York, 1975.

[Duf82] M. G. Duffy, *Quadrature over a pyramid or cube of integrands with a singularity at a vertex*, SIAM J. Numer. Anal. **19** (1982), no. 6, 1260–1262.

[Ee92] T. O. Espelid and A. Genz (eds.), *Numerical integration: recent developments, software and applications*, NATO ASI Series, vol. 357, Kluwer Academic Publishers, London, 1992.

[ES96] A. Erichsen and S.A. Sauter, *Efficient automatic quadrature in 3-d Galerkin BEM*, Tech. Report TR-96-15, Berichtsreihe des Mathematischen Seminars Christian-Albrechts-Universität zu Kiel Ludewig-Meyn-Str. D-24098 Kiel, 1996.

[Evg66] M.A. Evgrafov, *Analytic functions*, W.B. Saunders Company, 1966.

[Fin96] D. Finocchiaro, *Monte carlo evaluation of electrostatic potential and potential energy*, Tech. Report TR-IMC B4-96-12, Istituto di Matematica Computazionale del CNR, Via Santa Maria 46, Pisa, Italy, 1996.

[Geo91] K. Georg, *Approximation of integrals for boundary element methods*, SIAM J. Sci. Stat. Comput. **12** (1991), no. 2, 443–453.

[GGM93] A. Greenbaum, L. Greengard, and G.B. McFadden, *Laplace's equation and Dirichlet-Neumann map in multiply connected domains*, J. of Comp. Phys. **105** (1993), 267–278.

[GR87] L. Greengard and V. Rokhlin, *A fast algorithm for particle simulations*, Journal of Computational Physics **73** (1987), 325–438.

[Gre88] L.F. Greengard, *The rapid evaluation of potential fields in particle systems*, The MIT Press, 1988.

[Gue92] J. Guermond, *Numerical quadrature for layer potentials over curved domains in R^3*, SIAM J. Numer. Anal. **29** (1992), 1347–1369.

[HLS95] W. Hackbusch, C. Lage, and S.A. Sauter, *On the efficient realization of sparse matrix techniques for integral equations with focus on panel clustering, cubature and software design aspects*, Tech. Report 95-4, Berichtsreihe des Mathematischen Seminars Christian-Albrechts-Universität zu Kiel Ludewig-Meyn-Str. D-24098 Kiel, 1995.

[HS93] W. Hackbusch and S.A. Sauter, *On the efficient use of the Galerkin-method to solve Fredholm integral equations*, Applications of mathematics **38** (1993), 301–322.

[Jac75] J. Jackson, *Classical electrodynamics*, Wiley, New York, 1975.

[KE97] P. Keast and G. Fairweather (Eds.), *Numerical integration: recent developments, software and applications*, NATO ASI Series, vol. 203, Kluwer Academic Publishers, London, 1997.

[LC94] J. N. Lyness and R. Cools, *A survey of numerical cubature over triangles*, Proceedings of Symposia in Applied Mathematics, vol. 48, American Mathematical Society, 1994, pp. 127–150.

[LL80] L.D. Landau and E. M. Lifshitz, *The classical theory of fields*, Pergamon Press, Oxford, 1980.

[LM80] J. N. Lyness and G. Monegato, *Quadrature error functional expansions for the simplex when the integrand function has singularities at vertices*, Mathematics of Computation **34** (1980), no. 149, 213–225.

[Lyn76] J. N. Lyness, *An error functional expansion for N-dimensional quadrature with an integrand function singular at a point*, Mathematics of Computation **30** (1976), no. 133, 1–23.

[Lyn78] J. N. Lyness, *Quadrature over a simplex. II. A representation for the error functional*, SIAM Journal on Numerical Analysis **15** (1978), no. 5, 870–887.

[May92] A. Mayo, *The rapid evaluation of integrals of potential theory on general regions*, J. Comp. Phys. **100** (1992), 236–245.

[MGM95] A. McKenney, L. Greengard, and A. Mayo, *A fast Poisson solver for complex geometries*, J. Comp. Phys. **118** (1995), 348–355.

[Nie92] Harald Niederreiter, *Random number generation and Quasi-Monte Carlo Methods*, CBMS-NSF regional conference series in Appl. Math., vol. 63, SIAM, Philadelphia, 1992.

[Pel96] M. Pellegrini, *Electrostatic fields without singularities: Theory and algorithms*, Proceedings of the 7th ACM-SIAM Symposium on Discrete Algorithms, 1996, Extended version in Tech Report IMC B4-96-02, Istituto di Matematica Computazionale del CNR, Via Santa maria 46, Pisa, pp. 184–191.

[Pel97] M. Pellegrini, *Monte carlo approximation of form factors with error bounded a priori*, Discrete & Computational Geometry **17** (1997), 319–337.

[PRT92] V.Y. Pan, J.H. Reif, and S.R. Tate, *The power of combining the techniques of algebraic and numerical computing: Improved approximate multipoint polynomial evaluation and improved multipole algorithms*, Proceedings of the 33rd Annual Symposium on Foundations of Computer Science, 1992, pp. 703–713.

[Rok83] V. Rokhlin, *Rapid solution of integral equations of classical potential theory*, J. Comp. Phys. **60** (1983), 187–207.

[San76] L. A. Santaló, *Integral geometry and geometric probability*, Addison-Wesley, Reading, MA, 1976.

[Sch94a] C. Schwab, *On numerical cubature of nearly singular surface integrals arising in BEM collocation*, Computing **52** (1994), 139–159.

[Sch94b] C. Schwab, *Variable order composite quadrature of singular and nearly singular integrals*, Computing **53** (1994), 173–194.

[Sch95] C. Schwab, *Boundary layer resolution in hierarchical plate modelling*, Mathematical methods in Applied Sciences **18** (1995), 345–370.

[SK96] S.A. Sauter and A. Krapp, *On the effect of numerical integration in the Galerkin boundary element method*, Numerische Matematik **74** (1996), 337–359.

[SS96] S.A. Sauter and C. Schwab, *Quadrature for hp-Galerkin BEM in 3-d*, Tech. Report TR-96-02, Seminar for Applied mathematics, Department of Mathematics, ETH, Zurich, 1996, To appear in Numerishe Matematik.

[Str71] A.H. Stroud, *Approximate calculation of multidimensional integrals*, Pretince-Hall, Englewood Sliffs, New Jersey, 1971.

[SW92a] C. Schwab and W.L. Wedland, *Kernel properties and representation of boundary integral operators*, Math. Nachr. **156** (1992), 187–216.

[SW92b] C. Schwab and W.L. Wedland, *On numerical cubature of singular surface integrals in boundary element methods*, Num. Math. **62** (1992), 343–369.

[vPS96] T. von Petersdorff and C. Schwab, *Fully discrete multiscale Galerkin BEM*, Tech. Report TR-95-08, Seminar for Applied mathematics, Department of Mathematics, ETH, Zurich, 1996.

[Zha87] Feng Zhao, *An O(N) algorithm for three-dimensional N-body simulations*, Tech. Report AITR-995, Artificial Intelligence Laboratory, Massachusetts Institute of Technology (MIT), Cambridge, Massachusetts, October 1987.

[Zho93] P.B. Zhou, *Numerical analysis of electromagnetic fields*, Springer Verlag, 1993.

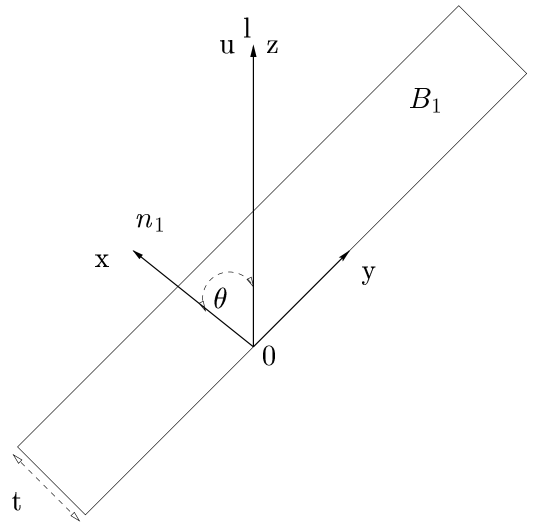

Figure 1: Geometric setting for B_1: cross-section at $\eta = 0$.

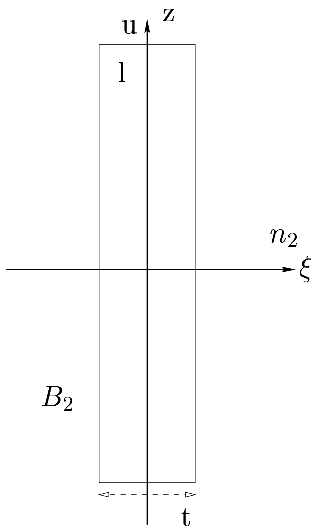

Figure 2: Geometric setting for B_2: cross-section at $\eta = 0$.

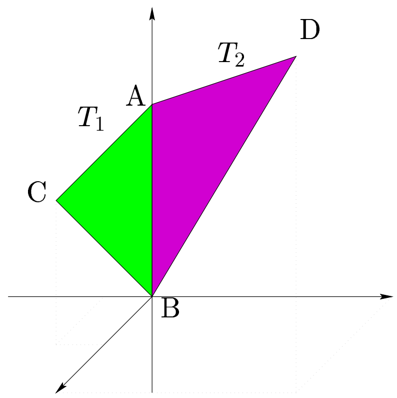

Figure 3: Two triangle is 3-space sharing an edge.

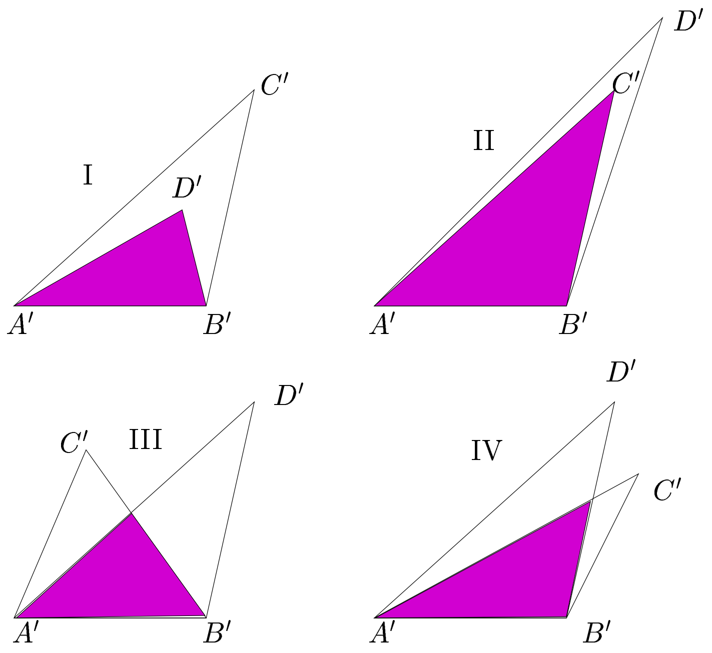

Figure 4: Four different combinatorial types of projections.

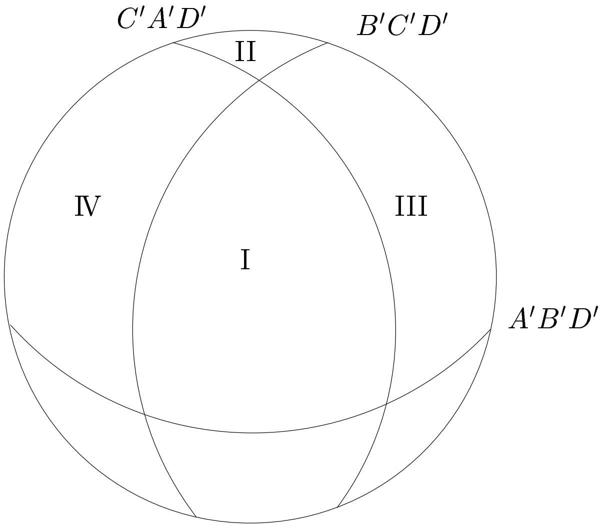

Figure 5: Four relevant regions on the sphere.

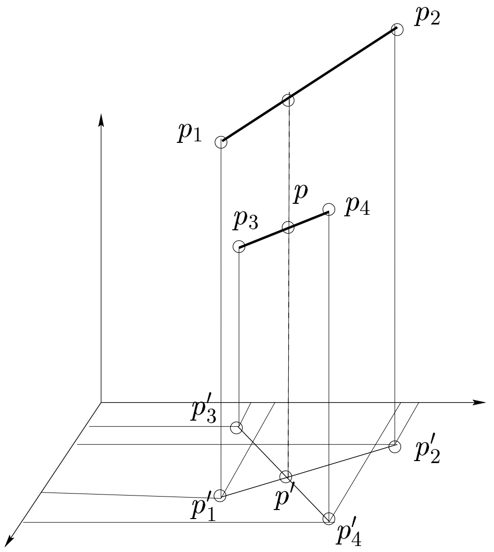

Figure 6: Intersection point p' as projection of point p.

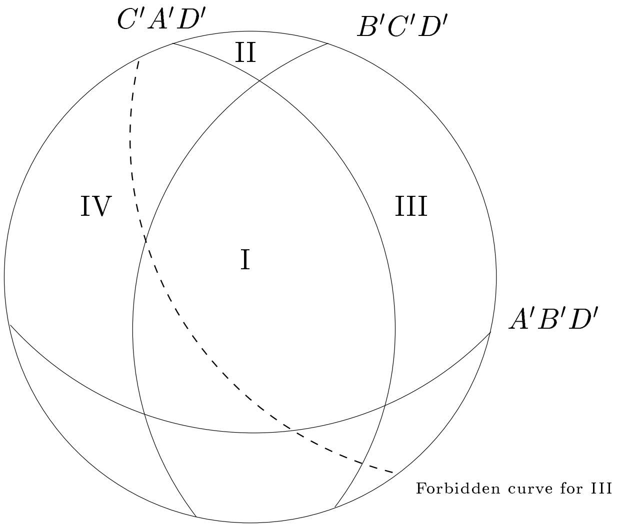

Figure 7: Forbidden curve of region III.

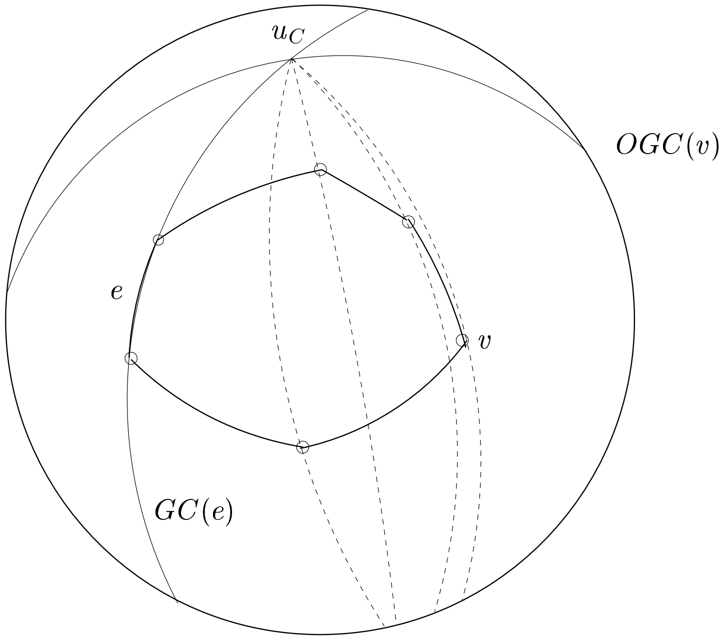

Figure 8: Slicing of a spherical polygon into sub-regions.

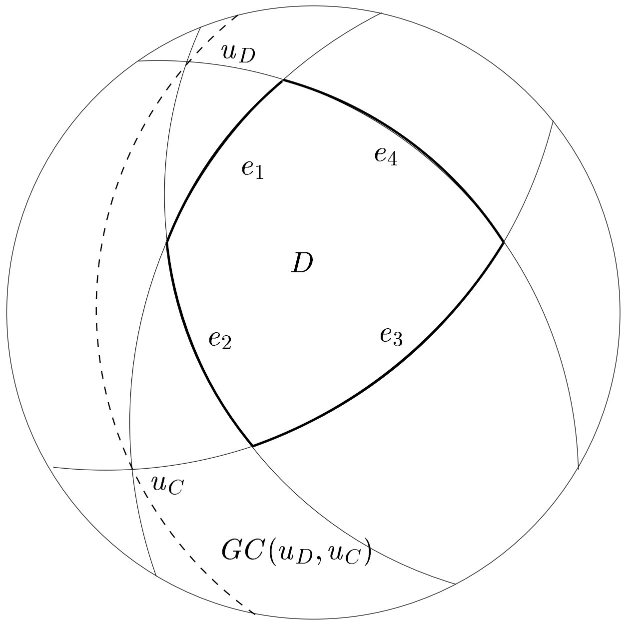

Figure 9: Determination of points u_C and u_D for a spherical quadrilateral.

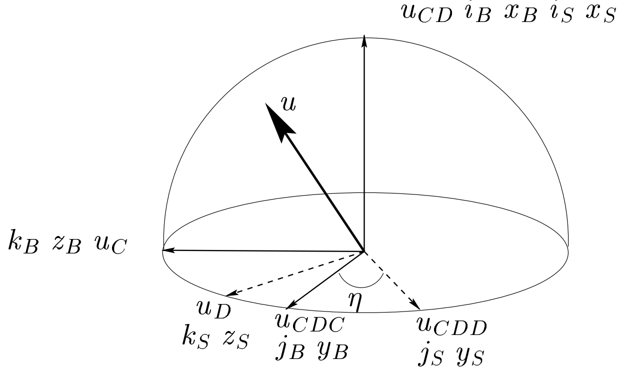

Figure 10: Construction of Base reference and Slanted reference frames.

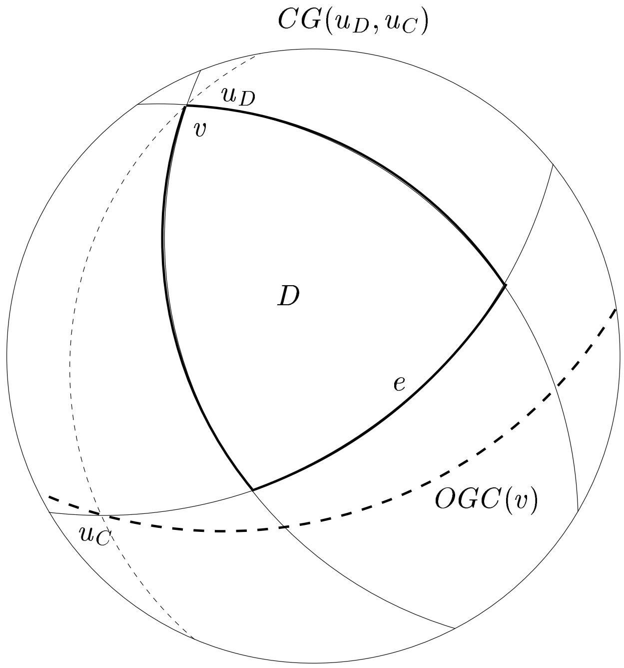

Figure 11: Determination of points u_C and u_D for a spherical triangle.

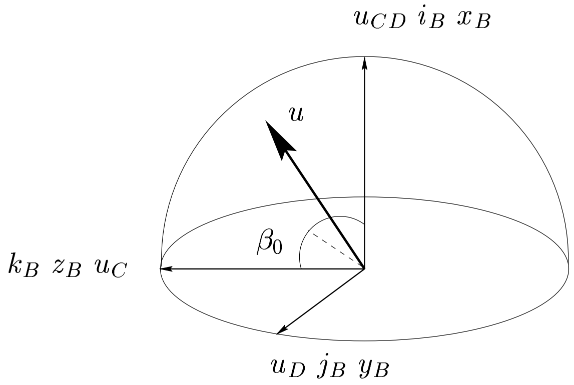

Figure 12: Construction of Base reference frame and angle shift.

Directions	$A = \pi/32$	$A = \pi/16$	$A = \pi/8$	$A = \pi/4$	$A = \pi/2$	$A = 3/4\pi$
24	(1)124	(2)793	(2)161	(2)224	(2)228	(2)189
54	(2)482	(2)191	(5)642	(3)377	(3)208	(3)151
96	(2)174	(3)401	(4)564	(4)515	(4)154	(5)961
216	(3)217	(4)111	(5)553	(6)978	(7)102	(7)417
486	(5)845	(6)468	(7)803	(9)269	(10)601	(10)126
1014	(8)299	(8)122	(9)258	(12)166	(13)15	(14)1
1536	-	(9)587	(11)671	(12)995	(13)12	-

Table 1: Number of Directions / Relative Error

Seconds	$A = \pi/32$	$A = \pi/16$	$A = \pi/8$	$A = \pi/4$	$A = \pi/2$	$A = 3/4\pi$
0.01	(1)124	(2)793	(2)161	(2)224	(2)228	(2)189
0.02	(2)482	(2)191	(5)642	(3)377	(3)208	(3)151
0.05	(2)174	(3)401	(4)564	(4)515	(4)154	(5)961
0.1	(3)217	(4)111	(5)553	(6)978	(6)102	(7)417
0.2	(5)845	(6)468	(6)336	(7)189	(10)601	(10)126
0.5	(7)299	(8)447	(9)258	(12)166	(13)11	(14)1
0.9	(8)157	(10)321	(11)342	-	-	-

Table 2: Seconds / Relative Error

Directions	$B = \pi/6$	$B = 2/6\pi$	$B = 3/6\pi$	$B = 4/6\pi$	$B = 5/6\pi$
24	(3)735	(2)308	(2)643	(2)941	(1)109
54	(4)295	(3)480	(3)546	(2)118	(2)192
96	(3)129	(4)334	(4)999	(3)235	(3)52
216	(5)192	(5)101	(5)242	(5)925	(4)387
486	(7)473	(8)282	(7)108	(7)792	(6)802
1014	(10)212	(12)44	(11)86	(9)149	(8)486

Table 3: Number of Directions / Relative Error

Seconds	$B = \pi/6$	$B = 2/6\pi$	$B = 3/6\pi$	$B = 4/6\pi$	$B = 5/6\pi$
0.01	(3)735	(2)308	-	(2)941	(1)109
0.02	(4)295	(3)48	(2)643	(2)118	(2)192
0.05	(3)129	(4)334	(4)999	(3)235	(3)52
0.1	(5)192	(5)101	(5)242	(5)925	(4)387
0.2	(7)473	(8)282	(7)108	(7)792	(6)802
0.5	-	(11)616	(11)144	(10)378	(8)194

Table 4: Seconds / Relative Error

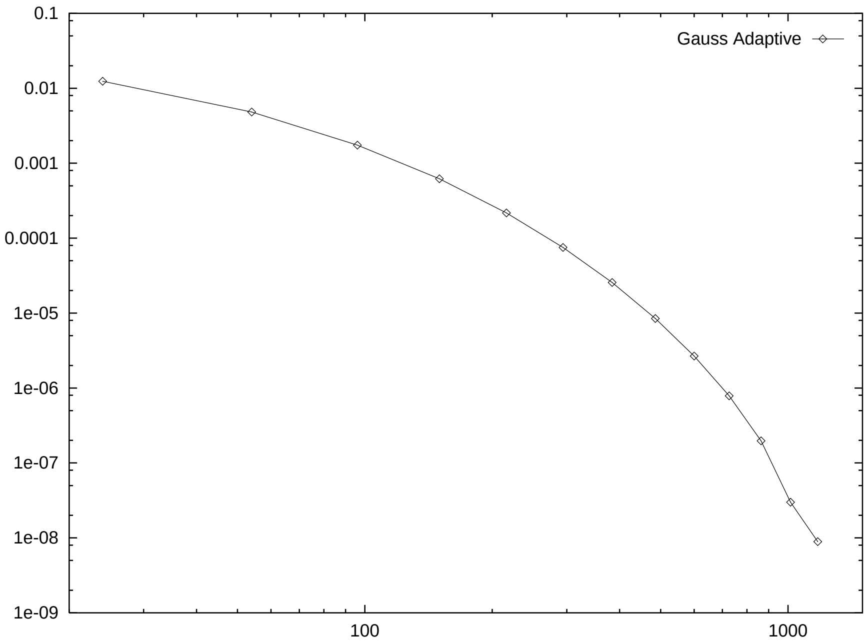

Figure 13: $A = \frac{\pi}{32}$; Directions/relative error

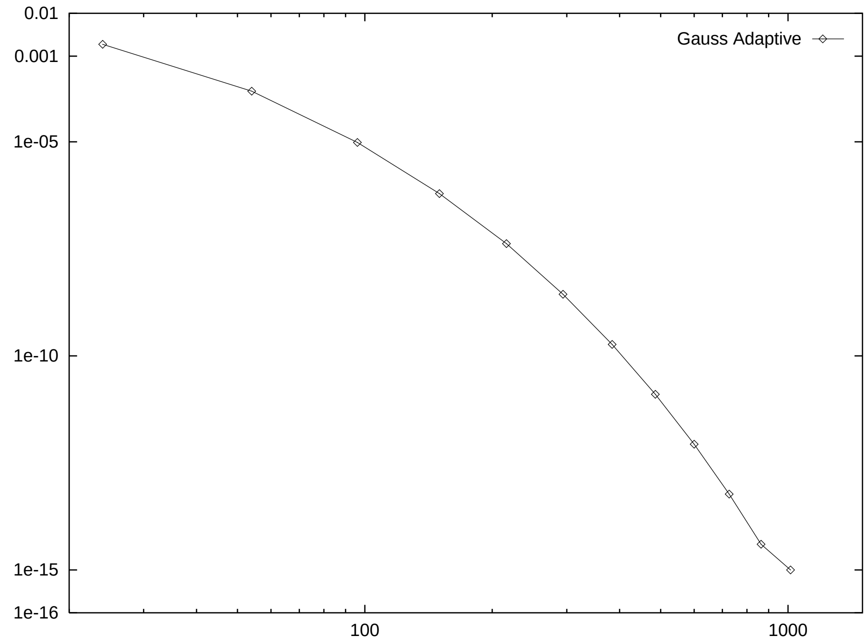

Figure 14: $A = \frac{4\pi}{3}$; Directions/relative error

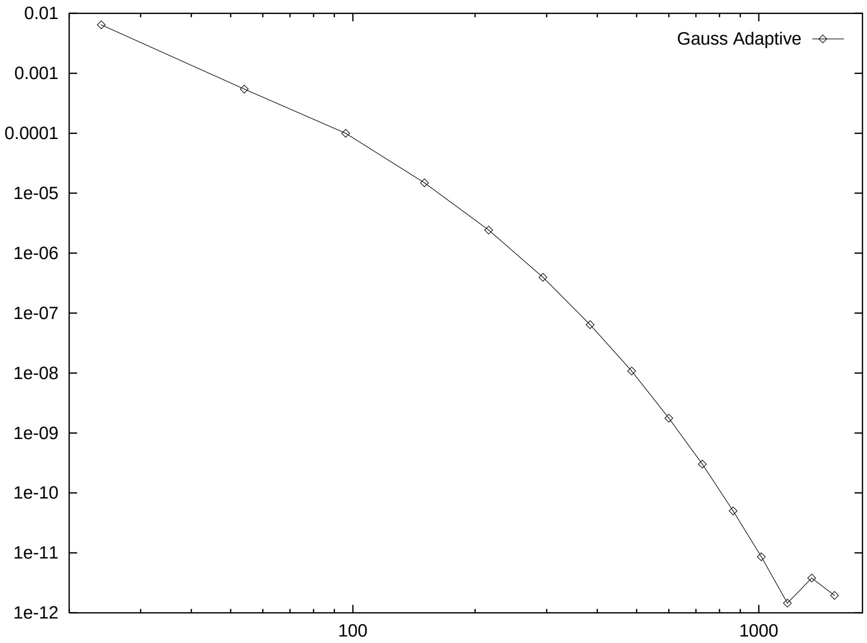

Figure 15: $B = \frac{3}{6}\pi$; Directions/relative error

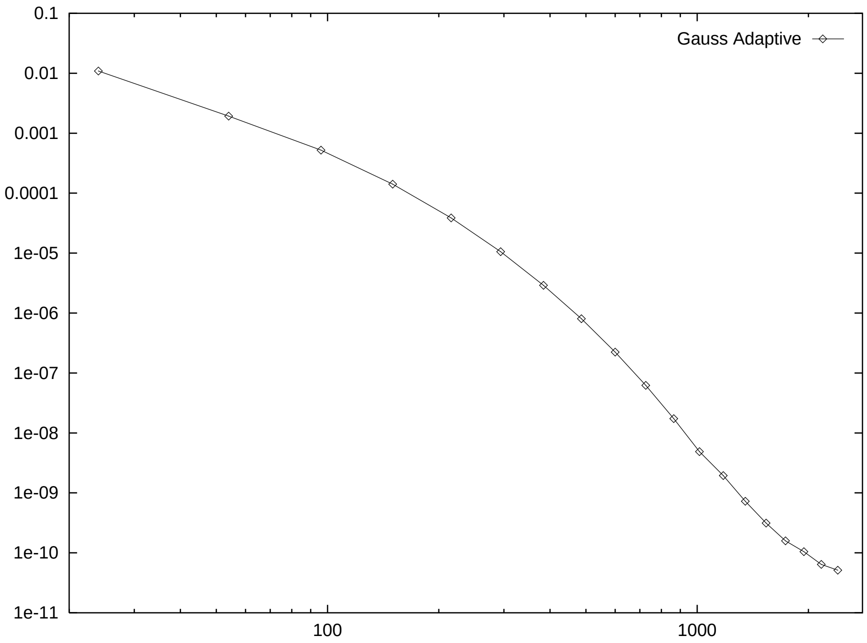

Figure 16: $B = \frac{5}{6}\pi$; Directions/relative error